CHAPTER 7

Spatial Scaling Methods for Landscape and Regional Ecosystem Analysis

I. INTRODUCTION

Representing the variability of a typical landscape quantitatively is a daunting task. The most common source of spatial information for land management has historically been recorded on maps. Explorers denoted only rivers, mountains, and related landscape features along their routes. Later, the locations of roads, rail lines, and towns were added. In time, specialists made surveys of the types of vegetation and soils present, and mapped major drainage patterns. All of these properties represented what could be directly observed and quantified from a small number of samples. The means of these samples were then extrapolated, with the aid of aerial photographs and topographic maps, to fill entire maps.

Today's landscape analysis requires maps with additional features that are not directly observable. These include estimates of the stores of water, carbon, and nutrients in vegetation and the soil, as well as the cycling rates of various ecosystem processes. In addition, landscape and regional scale ecosystem analysis must document on maps those processes that cause changes in the spatial distribution of flora and fauna, such as the rate and

direction of seed dispersal, animal population dynamics, and the spread of wildfires and other disturbances. A fundamental problem is that we cannot rely on the same field techniques that were satisfactory for stand-level analyses; rather, we must relate features that can be obtained from stand-level analyses to more observable landscape features based on completely different methods.

This chapter introduces a number of methods borrowed from other disciplines that have proved valuable, in fact, essential, to conduct broader scale ecosystem analysis. These new methods include application of geographic information system techniques, database management, climatological extrapolations, and remote sensing. We present a brief explanation of each of the major fields, along with some underlying principles that permit them to contribute so essentially to landscape and regional scale analyses. References are provided for those interested in developing special skills in these areas. Applications at the landscape and regional scales will be presented in Chapters 8 and 9.

A. Landscape Patterns and Processes

There is no single approach appropriate for the ecological analysis of landscapes. Different questions require that different variables be estimated at varying space and time scales (Levin, 1992). At a more fundamental level, landscape analysis questions differ dramatically in the level of spatial *interconnectedness* required. Figure 7.1 shows a raster representation of a hypothetical landscape in a grid system with a "target cell" in the center. As an organizing principle, we can think of three dimensions of connectivity around the target cell. The cell is connected vertically upward to the atmosphere, vertically downward with the soil, and horizontally with adjacent ecosystem units. As we simplify our view of the landscape, we may choose to define some of these dimensions weakly, while ignoring others entirely. Such simplifications are necessary to accomplish landscape analysis, but they must be made to accommodate the problem being addressed. The additional dimension of "time" must also be considered along with the three dimensions of connectivity.

Some questions in ecosystem analysis can be dealt with by evaluating the vertical connections of the target cell only, such as those concerned with vegetation and atmospheric interactions through the application of Soil–Vegetation–Atmospheric Transfer (SVAT) models. For example, estimating NPP with a Light Use Efficiency (LUE) model (Chapter 3) requires for a given target cell only knowledge of the incident radiation, the light absorbing capacity of the canopy, and the conversion efficiency of the absorbed radiant energy into biomass. Except for rare cases of topographic shading, properties of the adjacent cells have little impact on the target cell, which permits estimates of NPP to be considerably simplified. When applying this "unconnected" logic, each cell can be evaluated individually, in any order. The earliest regional photosynthesis maps were assembled following this approach (Running *et al.*, 1989).

The spatial connectiveness must be expanded, however, if we ask the question, "How favorable is the wildlife habitat in a specified cell?" To answer this question we must obtain information on forage quality and cover present within a target cell as well as in adjacent cells with other critical attributes that affect wildlife populations: locations of water, breeding grounds, predator populations, roads, and other barriers or distractions associated with human activities. Continuing this line of reasoning, one can pose ecologi-

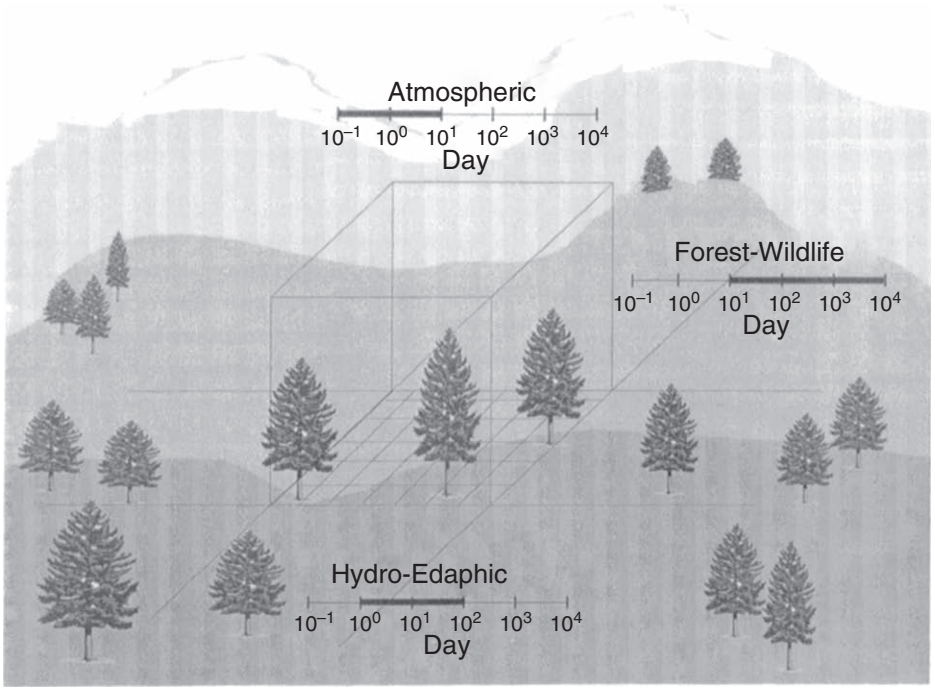

FIGURE 7.1. Principles of landscape interconnections. Each landscape cell is connected vertically above to the atmosphere, below to hydroedaphic processes, and horizontally to adjacent terrestrial cells. Key ecosystem processes and the inherent time constants (darkened line) vary for these different spatial dimensions. Simplifying regional scale analyses requires that only the essential connective processes be defined.

cal questions associated with animal migration or fire spread where connectiveness beyond adjacent cells is required. The amount of information required to relate properties in the target cell with adjacent (and even distant) landscape cells adds complications to spatial analysis in a geometric way. There is great merit, therefore, in simplifying the degree of interconnectedness by identifying properties that might be ignored in a particular analysis. For example, in a wildlife habitat survey, one might minimize evaluation of the vertical atmospheric and hydrologic connections, and define only a handful of more stable attributes of the vegetation.

Hydrologic analyses of whole watersheds were among the first problems in forestry, beyond road location, that required explicit information from horizontally connected cells. Hydrologists originally dealt with landscape complexity by concentrating on the stream network and properties of the soil that affected seepage and runoff. Vegetation was usually treated as a static evaporating surface without any explicit connection to the hydrologic properties of adjacent cells. Stream discharge was of primary interest; most other ecosystem processes were thus ignored. In Chapter 8 we will cover recent projects that incorporate vegetation processes interactively to simulate streamflows with changing vegetation.

We can recommend some general steps when beginning a regional ecosystem analysis. First, obtain an inventory of what is on the landscape, and where it is located. This step is akin to evaluating the state of the system at one point in time. A second step involves describing what features may be inferred spatially from data acquired through remote sensing and related techniques. We soon appreciate that attributes commonly measured by foresters and botanists, such as variation in tree diameters and species compositions, cannot be measured over thousands of square kilometers. Regional forest growth models must instead depend on relationships associated with climatological extrapolations and remotely sensed indices of vegetation greenness and LAI. A final step required in spatial analyses is to develop a means of inferring other variables of critical interest from the few variables that can be measured. This last step usually involves the application of a computer simulation model.

We begin in the following section to provide some rules for translating ecosystem properties into observable variables. Next we cover principles of remote sensing that define what ecosystem and climatic attributes are directly measurable across landscapes. Finally, we summarize the landscape metrics used to quantify landscape patterns, as a prelude to problems that require spatially explicit and dynamic landscape analysis with strong horizontal coupling.

B. Model Simplifications

Ecosystem analysis can safely progress to regional scales only when the principles underlying ecological processes are reasonably well understood and have been synthesized into some type of analytical model. In Chapters 2–6, we provided background on our current understanding of forest ecosystem operation and synthesized much of that understanding into models such as FOREST-BGC. With this background, we can, through sensitivity tests, discover the most critical variables and establish relationships for constructing more simplified models required to extrapolate selected information across landscapes (Burke *et al.*, 1991).

The first requirement of spatial scaling is to reduce the number of variables requiring measurement to a minimum. Early ecosystem models of the International Biological Program (IBP) era in the 1970s required so much information that they could not be extrapolated beyond the highly sampled sites on which they were developed. For example, the CONIFER model of the IBP Coniferous Biome project required information on 109 variables before it could be operated (Swartzman, 1979).

As FOREST-BGC evolved from its origins in the early 1970s, a number of system representations were tested and discarded in the search for a scalable model. Ultimately, five important simplifications were incorporated into the model:

- No demography of individual species was defined, only general physiological attributes.
- Individual trees were not represented, only carbon pools.
- No details on internal physiology concerning water, carbon, or nutrient transport were included. This decision resulted in compression of 16 specified water storage compartments from an earlier version of FOREST-BGC to 1 in the current model.

- No individual canopy strata were represented in FOREST-BGC, only total LAI. In contrast, some photosynthesis models define 8–10 vertical canopy strata, each age class of foliage, and additional physiological attributes (Wang and Jarvis, 1990).
- No belowground details on root distribution or variation in soil profile properties were represented. Root growth was computed as a simple "carbon tax" to meet the demands associated with the development of canopy LAI.

These types of simplifications, although unnecessary for stand-level models (see Korol *et al.*, 1995, 1996; Keane *et al.*, 1996a), are essential for landscape and regional scale analyses. Belowground ecosystem properties, difficult to measure under any circumstances, must be inferred at larger scales from correlations with modeled ratios of actual to potential GPP (see LUE models in Chapter 3) or similar derivations. Even the widely applied CENTURY model, which focuses explicitly on soil processes, computes soil carbon dynamics exclusively from aboveground climate, NPP, and the application of carbon cycling principles (Parton *et al.*, 1988, 1993). Kicklighter *et al.* (1994) simulated regional soil CO_2 fluxes by first using air temperature to estimate soil temperature, and then extrapolated an empirical relation between soil temperature and soil CO_2 efflux obtained from a few plots. Not surprisingly, no example exists where regional analyses of CO_2 fluxes and changes in carbon storage have been able to include detailed information on belowground processes.

The final objective of system simplification is to identify a small set of critical but *observable* system attributes, and key environmental variables that affect them. The model, when complete, still must be able to compute important physiological processes across landscapes. It is essential that the steps in model simplification proceed hand in hand with evaluation of the technology available to make measurements and analyze the results. For example, we chose canopy LAI as a key property of the vegetation for inclusion in FOREST-BGC because LAI is an excellent reference on which to base calculations of CO_2 and water vapor exchange (including surface evaporation), and because it can be assessed at an adequate level of spatial and temporal resolution with present satellite sensors. Other more classic forestry measures such as stem basal area and live-crown ratio neither provide the direct relationship to canopy processes nor can be remotely sensed with present technology.

In summary, we recommend a specific order in compiling data for landscape analyses: (1) Begin with the most stable and available types of data, namely, topography and soil maps. (2) Next, acquire climatic data needed to drive most types of ecosystem models. (3) Finally, obtain information on the more dynamic properties, such as the vegetation. The flow diagram represented in Fig. 7.2 identifies major types of data sets and their sources. From these basic data sets techniques are available to convert the primary information into forms that can be modeled and displayed in a geographic information system (GIS). The spatially organized data are further transformed through a series of specialized simulation models into ecosystem projections of carbon, water, and nutrient cycling across landscapes and regions to answer different types of questions. The most stable variables are those listed under the broad headings of topography and soils. Climatic data are usually archived in a form that can be used to drive most ecosystem models. Attributes of the vegetation are most difficult to obtain because satellite imagery must be acquired and the

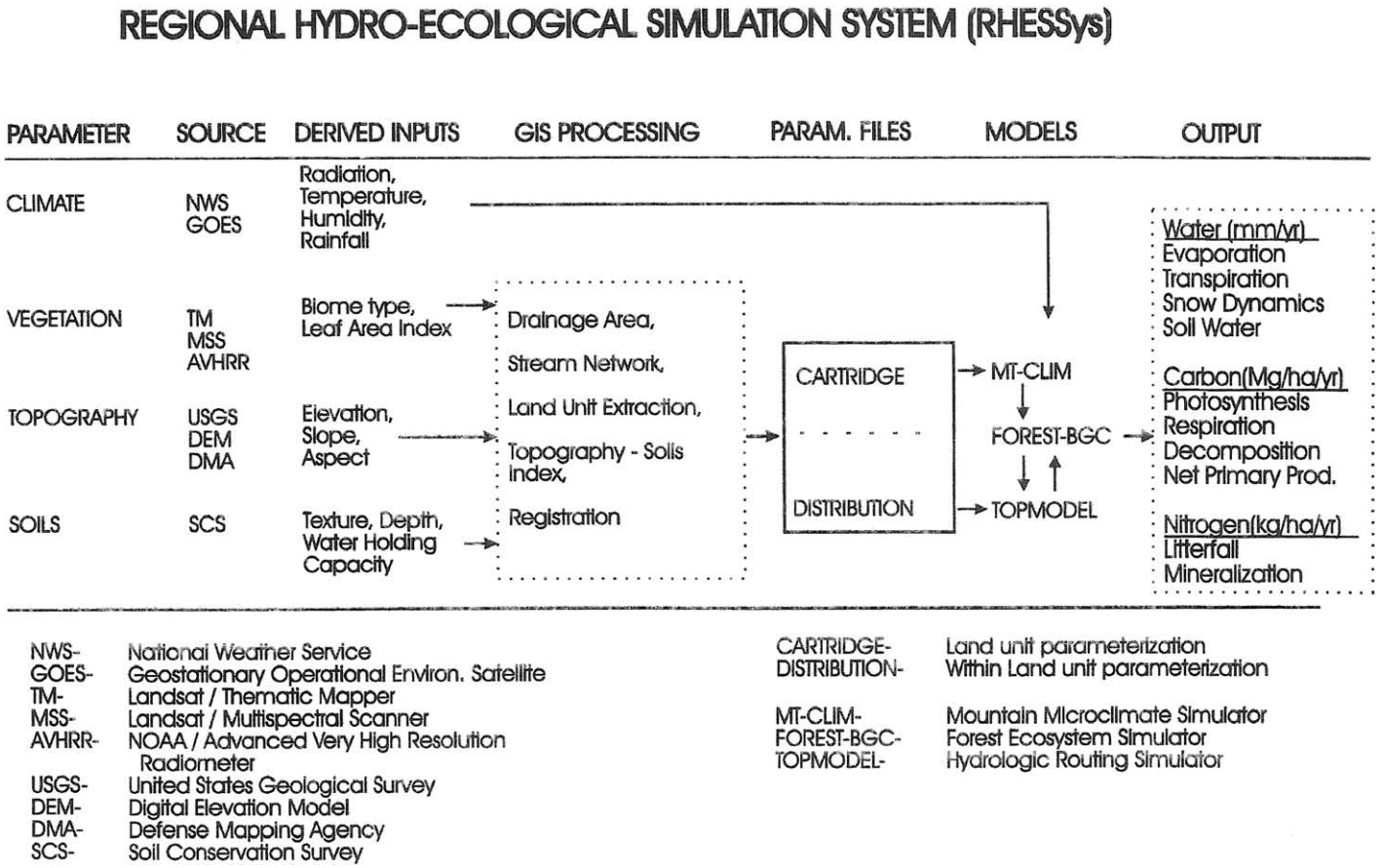

FIGURE 7.2. Integration of data layers of physical and biological characteristics of a landscape with process models to yield key ecosystem responses for the Regional Hydroecological Simulation System (RHESSys) (Band *et al.*, 1991, 1993). An earlier, simpler version of the Regional Ecosystem Simulation System (RESSys) does not incorporate TOPMODEL horizontal hydrologic connections (Running *et al.*, 1989).

reflectance properties from various electromagnetic bands must be translated into defined biotic properties, such as LAI.

II. ABIOTIC SITE VARIABLES

A. Principles in Geographic Representation

The simplest mathematical representation of a landscape is accomplished by overlaying a grid of square cells with equal dimensions, known as a *raster* format. Any cell within the grid can be addressed in a computer database by simply defining the *x* and *y* coordinates. With any raster GIS package, the size of the cell is arbitrary, so, in principle, any landscape could be defined within a raster database to any degree of accuracy. This approach would likely result in an exceedingly large database. The Landsat Thematic Mapper (TM) with 30×30 m pixel dimensions is often used as a cell size, but describing the 1200-km^2 Seeley–Swan basin in Montana at 30 m resolution would require 1.3 million raster cells. Alternatively, polygons of any shape can serve to define the landscape in what is called a *vector* format. Cell identification within a vector database is more difficult than in a raster format, but a vector format more realistically represents complicated landscape patterns.

Regardless of the spatial representation chosen, the goal is to partition the landscape into cells that maximize both the homogeneity of ecosystem properties within each cell and the heterogeneity between cells. In practice, properties most useful for landscape partitioning are either site variables, such as topographic discontinuities represented by ridge tops, hydrologic drainage paths, and local climate, or distinct variation in plant life forms, such as forests and grasslands. Ideally, a landscape mosaic of forest and grasslands can be defined by a set of homogeneous forest cells intermingled with homogeneous grassland cells. In reality, this clear representation is impossible because transitional situations exist.

1. Topography

Of the many sources of landscape heterogeneity, topography is the probably most important, because it influences both the local climate and hydrologic drainage. It is also most directly quantified. Stratification of the terrain into units with small internal topographic variation in aspect, slope, and elevation is accomplished by building the watershed structure from gridded digital elevation data. Band (1989a,b) developed computer programs that read the raw file of elevation data points into a digital elevation model (DEM). Then, beginning at the lowest point of the landscape, the model progressively computes the area above that will drain into the cell at the bottom of the specified area. When the program completes conputation of a landscape, each watershed is partitioned into uniquely defined hill slopes of specific slope and aspect, from which the hydrologic routing pattern is then produced. The threshold area specification allows a user to vary the level of topographic detail described in the final maps of the watershed. This important capability allows one to zoom in to obtain high detail from subdivisions of a watershed, or to pan out to a coarser description of an entire drainage basin. In this way, Nemani *et al.* (1993a) were able to represent the 1200-km^2 Seeley–Swan basin of Montana at varying degrees of topographic

complexity from 170 land units aggregated down to only 6 land units within the same RHESSys modeling system (see Plate 1).

Although the precise computations may differ, nearly all hydrologic analyses now make use of digital elevation data to construct a topographic template (Fairfield and Leymarie, 1991; Paniconi and Wood, 1993; Wigmosta *et al.*, 1994). Software packages for geographic information systems usually contain programs to compute landscape topography and define hill slope units with similar slopes and aspects. The accuracy of these topographic analyses is dependent on the scale and accuracy of the original DEM database. In many countries DEM data are available at 30 m horizontal and 1 m vertical resolution. In some parts of the world, however, only data with 1000 m horizontal and 100 m vertical resolution are available. Spatially coarse DEM data may still represent overall topography well enough to map local climatic variation, but they may be unable to depict the hydrologic networks correctly because small hills and streams were not shown in the original DEM data.

2. Hydrologic Routing

The first essential set of calculations in a hydrologic model involves the accurate computation of the terrestrial water balance, as presented in Chapter 2. A second set of critical calculations are those that deal with lateral flow of excess water from the land surface and subsurface soils into and through the stream channels, an example of horizontal connectiveness. In the earliest raster-based RESSys model, a simple "bucket" analogy from FOREST-BGC was applied to calculate changes in soil water content. When precipitation filled the bucket, excess water was spilled into surface outflow or into groundwater. No attempt was made to model the lateral flow of water into adjacent landscape cells (Running *et al.*, 1989). Although this simple bucket model proved adequate in areas of low relief with little lateral drainage, in mountainous areas explicit soil water routing proved necessary to produce realistic soil moisture profiles across a watershed and to predict streamflow.

The most direct approach to define hydrologic routing is to connect all landscape units to one another. Wigmosta *et al.* (1994) presented an example with a raster-based landscape representation where each square cell was connected to eight adjacent cells. Those cells located at higher elevation than the reference cell defined a potential source of water, whereas those located below it became receptors for any flow out of the cell. Models using vector or polygon representations on a landscape make for efficient computations and result in a reasonable depiction of the flow of water downhill to the boundary of a watershed (Michaud and Sorooshian, 1994). Robinson *et al.* (1995) illustrated that in small watersheds the hydraulic conductivity of hill slope cells plays an important role in determining variation in streamflow, but as the area increases, good definition of the stream network becomes more important. If the scale of analyses is restricted to upland forested watersheds, soil depth and hydraulic conductivity of hill slope cells must be well represented. At the scale of drainage basins, however, the priority shifts toward assuring accurate definition of the stream network.

The TOPMODEL logic of Beven and Kirkby (1979; Beven, 1989) offered an improvement in computational efficiency by developing equations that aggregate areas into zones

with similar hydrologic properties. TOPMODEL calculates the upslope drainage area and slope gradient for any hill slope unit and provides an estimate of the saturated flow rate through the soil from that unit. These soil drainage characteristics can either be defined for each hill slope unit or expressed as a frequency distribution for the entire watershed. For example, an area near a ridge top receives little drainage from upslope and would characteristically be situated on steep topography with shallow, coarse soils. Precipitation will rapidly drain downslope from such a location, leaving soils at moisture conditions below saturation most of the time. At the other extreme, an area at the base of the slope area, situated on gentle topography, continues to receive water from uphill sources most of the time and remains near saturation for long periods. Band *et al.* (1993) developed a Topographic Saturation Index (TSI) that spatially distinguishes all hill slope units possessing similar hydrologic flow characteristics in order to substantially reduce the number of computations required (see Plate 2). Daily outflow from any hill slope unit was calculated based on the TSI of each cell, the current soil saturation deficit, and the soil's saturated hydraulic conductivity (Nemani *et al.*, 1993b). This simplified TOPMODEL logic computes seasonal streamflow with accuracy equal to that achieved by more explicit hydrologic routing schemes on mountain watersheds (Franchini *et al.*, 1996; Moore and Thompson, 1996).

The evolution of early regional hydrologic analyses from a simple, raster-based, bucket model to the RHESSys, with more realistic representation of watershed drainage properties, is primarily the result of developing an automated scheme for partitioning the topography into functionally similar units and integrating that information into a hydrologic routing routine. This approach serves two important roles: it provides good estimates of watershed capacitance, which greatly improves accuracy in estimating the timing and volume of stream discharge, and it represents realistically how soil moisture is distributed across landscapes. This latter attribute is important because geologically unstable slopes are identified, and ecosystem model predictions of gas exchange from soils and vegetation supplemented by seepage from uphill positions are improved.

3. Soil Characteristics

Soil variables are among the most difficult ecosystem properties to quantify because of local heterogeneity and the deficiency of broad scale data. Georeferenced databases of soil morphological and structural characteristics are becoming available to resource managers in some countries. In the United States, the National Soil Geographic Date Base (NATSGO) and State Soil Geographic Data Base (STATSGO) (USDA, 1991) provide national coverage and soils information for individual states. Ecological modeling, however, usually requires more specific soil physical and chemical information than are available from these summarized databases. Kern (1995a) tested different published formulas that use particle size distribution, bulk density, and soil organic matter data to derive soil water retention curves. Kern (1995b) then took particle size distribution, organic matter, rock content, and soil depth from the NATSGO database to define geographic patterns of soil water holding capacity for the contiguous United States. Kern's estimates are hard to validate at continental scales, but the research yields a consistent set of important variables for regional ecosystem analysis.

An alternative to statistically interpolated databases is to apply more fundamental geomorphic principles to construct detailed soil maps of watersheds. Zheng *et al.* (1996) used the STATSGO database and employed TOPMODEL to compute an index of topographic position, which was then used to infer soil depth and water holding capacity of the Seeley–Swan basin; the analysis later was expanded to apply to the entire state of Montana. Standard errors of estimates of water holding capacity derived with the topographic index were within 5 cm of values predicted in the STATSGO statistical database at both the watershed and statewide levels. Zheng *et al.* (1996) found, by applying geomorphic principles to define drainage patterns from DEM data, that a more logical spatial interpolation of soil depth resulted, with shallow soils concentrated near ridge tops and progressively deeper soils distributed toward the base of a slope. Zhu *et al.* (1996) made further improvements by applying fuzzy set theory and expert systems logic to refine the spatial distribution of soil survey data for a 400-km^2 forested area of Montana.

B. Efficient Landscape Representation

Statistical landscape representations provided by TOPMODEL analyses do not include the explicit interconnections required to represent spatial patterns related to fire spread, seed dispersal, or the distribution of wildlife. In part this is because the hydrologic system is driven by gravity, a variable less important to many other patterns observed on landscapes. In fact, fire spread is accelerated by upslope winds while convective winds inhibit downslope spread. Plate 1 illustrates again that a simple raster representation of a landscape at 30 m resolution produces more cells than can be efficiently analyzed. However, there is a danger also in choosing too large of a cell size because *aggregation errors* accumulate in the computations (Bartell *et al.*, 1988; Rastetter *et al.*, 1992). These errors have two primary causes: averages are derived from spatially diverse input variables (e.g., local climatic variation), and more nonlinear processes are averaged as the size of cells increases (Fig. 7.3).

The magnitude of aggregation errors is dependent on the spatial heterogeneity on the landscape of both abiotic (topography, soils, climate) and biotic variables (biome type, stand age, and cover distribution). Evaluating the significance of these aggregation errors is not easy because both the specific landscape and the output variable of interest must be designated. Turner *et al.* (1996) evaluated the aggregation errors propagated by describing a mountainous 55,000-km^2 region of Oregon with raster cells 1, 10, and 50-km on a side. Elevations ranging from 0 to 3000 m represented a large range in temperatures and precipitation that were continually averaged together as the width of cell size increased from 1 to 50 km (Fig. 1.4). Simulated NPP was 11% higher with the 50-km cells than at 1 km, but simulated hydrologic runoff was 45% lower. White and Running (1994) found that predictions of annual photosynthesis and evapotranspiration for a 450-km^2 mountain watershed differed by more than 15% with identical input data, depending on the choice of raster, polygon, or TOPMODEL landscape representation.

A common finding in these studies is that landscape aggregation may preserve mean values but progressively reduces the apparent variance (Band and Moore, 1995). A landscape aggregation that averages a north and south slope into a single cell may compute an accurate average NPP, but the actual variation between the slopes is lost. Consequently,

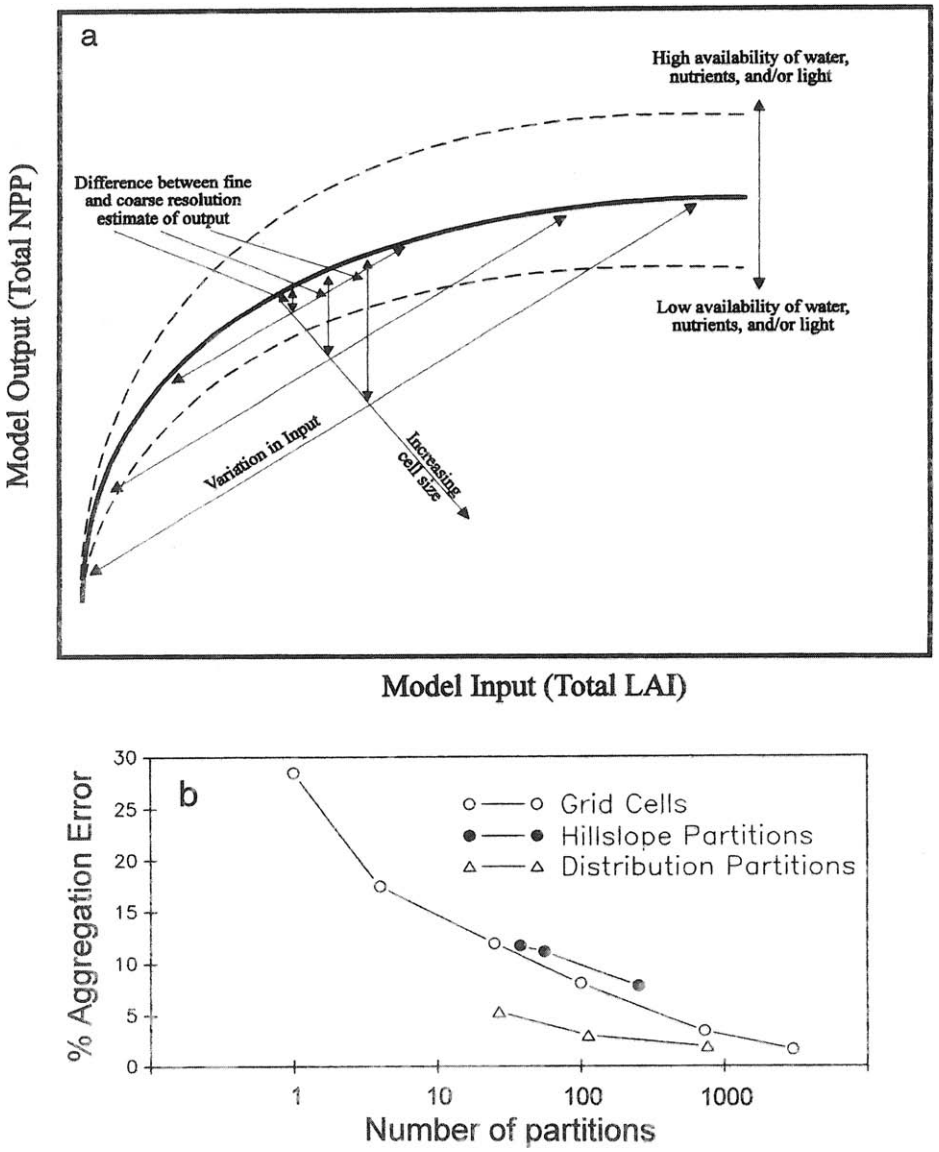

FIGURE 7.3. (a) Illustration of aggregation errors propagated by representing a landscape with progressively larger cells (Rastetter *et al.*, 1992). In this test, the relationship between LAI and NPP was nonlinear. If a landscape is represented with many cells over the full range of observed LAI, the estimation of NPP should be accurate. When the landscape is represented by progressively fewer aggregate cells assigned averaged LAI values, departure from the correct values increases. (b) The aggregation error in simulating NPP with RHESSys for a 12,100-km^2 region was reduced with smaller grid cell size. Topographically defined hill slope partitions improved the efficiency of computations (attaining a certain computational accuracy with the minimum number of cells) equal to grid cell representation. Landscape partitions defined by the distribution of LAI, soil water holding capacity, and precipitation provided the greatest efficiency. These variables were chosen for landscape classification based on previous understanding of their importance in affecting NPP in this region. (Redrawn from Pierce and Running, 1995.)

aggregated landscape computations may be adequate for general planning purposes but are usually not sufficiently accurate to make decisions regarding a specific site. Milne (1992) suggested that units with similar fractal geometry would share topographic properties and this could serve as a basis for selecting those cells that could be combined.

Pierce and Running (1995) studied the effect of both temporal (daily to annual simulations) and spatial variables (1–8456 partitions in both raster and polygon formats) on simulations of NPP over a 12,000-km^2 region in the northern Rocky Mountains. Landscape partitioning on the basis of three key input variables (LAI, soil water holding capacity, and precipitation) was found to be more efficient than topographic partitioning, and much more accurate than simple raster representation (Fig. 7.3). Coughlan and Running (1997b) developed from an expert system approach a means of partitioning forested landscapes based on key biophysical input variables for FOREST-BGC, such as LAI, that strongly influenced predicted output. In this way, they could assume before the model computation that the landscape units defined would be homogeneous in regard to the important variables. In all of these cases, the goal is to represent the landscape partitioning as accurately as possible, which produces more accurate results while reducing the number of redundant cells.

III. PROVIDING THE DRIVING VARIABLES, CLIMATOLOGY

We learned from Chapters 2–4 that the critical environmental driving variables for ecosystem analysis are incident solar radiation, air and soil temperature, humidity deficits, precipitation, and wind. Most ecological studies either collect the necessary data on site with a portable meteorological station or rely on archived climatological data from a nearby station. However, for regular execution of a regional ecosystem model a permanent source of consistent meteorological data is required. Again, compromises in the ecosystem model may be necessary to accommodate the realities of available regional data. An early version of FOREST-BGC (H2OTRANS) ran at hourly time steps (Running, 1984a; Knight *et al.*, 1985). The simplification to a daily time step model (DAYTRANS) was made primarily because there were no regularly archived hourly meteorological data available over large regions. The standard collection time for U.S. National Weather Service and World Meteorological Organization surface weather data is daily.

These standard weather data sources have two shortcomings for regional ecosystem analysis. First, most weather stations do not measure solar radiation, humidity, or wind speed. Second, the weather stations are located predominantly in valley bottoms, often at airports, and thus poorly represent the local climatic variability associated with complex terrain. To remedy these problems an array of climatological principles and formulas have been assembled into a computer model that allows nonlinear extrapolation of climatic data into mountainous terrain (MT-CLIM, Running *et al.*, 1987). Rather than reproduce the many equations in MT-CLIM here, we will discuss the principles on which the model is based. For those wishing to see the equations and other details, the complete documentation of MT-CLIM with computer code is available free at http://www.ntsg.umt.edu/textbooks/.

A. Climatology

1. Air Temperature

Canopy processes controlled by stomatal opening such as photosynthesis and transpiration are predominantly affected by air temperature during daylight hours. Other processes such as stem respiration occur continuously, so are best computed from integrated 24-hr average temperatures. The simple sine wave in MT-CLIM allows both these temperatures to be generated from daily minimum and maximum temperature data alone (Fig. 7.4). Although a sinusoidal variation in temperature is not typical every day, on average the assumption is valid.

2. Soil Temperature

Soil temperature is required for calculating most belowground ecosystem processes, including root growth and respiration, decomposition, and nitrogen mineralization. Soil temperature, however, is not a standard variable collected at most weather stations. Because soil temperature responds to the net effect of the daily surface energy balance, it can be estimated by computing a running average of air temperature, with progressively longer integration times as soil depth increases (Parton, 1984; Stathers *et al.*, 1985). Zheng *et al.* (1993) employed an 11-day running average air temperature, modified by daily precipitation and overstory LAI, to predict soil temperatures at 10 cm depth. When tested on sites across the United States, estimated soil temperatures were close to those observed (r^2 = 0.86–0.95).

3. Humidity

Climatological studies have long shown that nighttime air temperature typically cools until the dew point, T_{dew}, is reached. The resulting release of latent energy of vaporization (2454 kJ kg^{-1} at 20°C) usually inhibits further air temperature drop. MT-CLIM applies this simple principle to define daily dew point as equal to the minimum daily temperature, T_{min} (Fig. 7.4). This approach to calculating dew point is reasonably accurate, even in climates where dewfall does not regularly occur (Fig. 7.5; Glassy and Running, 1994; Running *et al.*, 1987). Kimball *et al.* (1997b) demonstrated a simple correction based on the ratio of annual precipitation to annual evapotranspiration (ET) that reduced the standard error of estimated vapor pressure to less than 0.4 kPa of measured values, even in arid climates (Fig. 7.6).

The dew point is an absolute measure of water vapor in an air mass. As such, it is not influenced by air temperature, so is fairly constant throughout the daily cycle. Because of the huge capacity of the atmosphere, daily surface evapotranspiration usually raises the water vapor concentration by only a small amount. Consequently, the dew point provides a conservative spatial and temporal measure of atmospheric water vapor. Other measures of humidity, such as the vapor pressure deficit (D), can then be calculated from T_{dew} and air temperature (Chapter 2).

4. Solar Radiation

Given the importance of solar radiation to meteorology, hydrology, and ecology, it is unfortunate that the network of weather stations generally disregards this variable. In

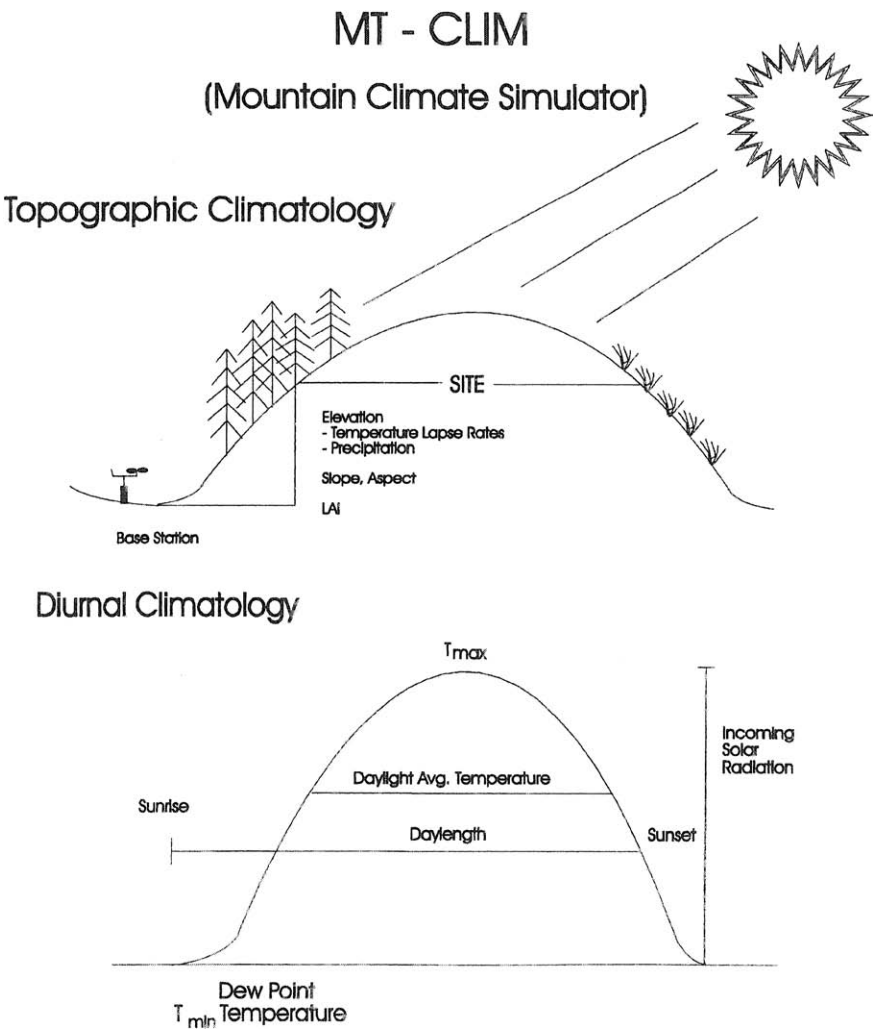

FIGURE 7.4. Depiction of principles behind the mountain microclimate simulator MT-CLIM to extrapolate daily meteorological data across topographically complex terrain and to compute ecologically relevant variables from daily maximum–minimum temperatures (Running *et al.*, 1987; Hungerford *et al.*, 1989). From diurnal extremes in temperature, the incident solar radiation, humidity, and soil temperature are derived. Solar radiation, precipitation, humidity, and air temperatures are further modified to take account of slope, aspect, elevation, and latitude.

MT-CLIM, a two-step approach is required to estimate solar radiation: first, potential solar radiation (often called top of the atmosphere solar radiation) is computed using solar geometry algorithms from Garnier and Ohmura (1968) and Swift (1976). These algorithms allow computation of direct beam potential radiation to a surface at any latitude for every day of the year. Then, by applying principles described in Bristow and Campbell (1984),

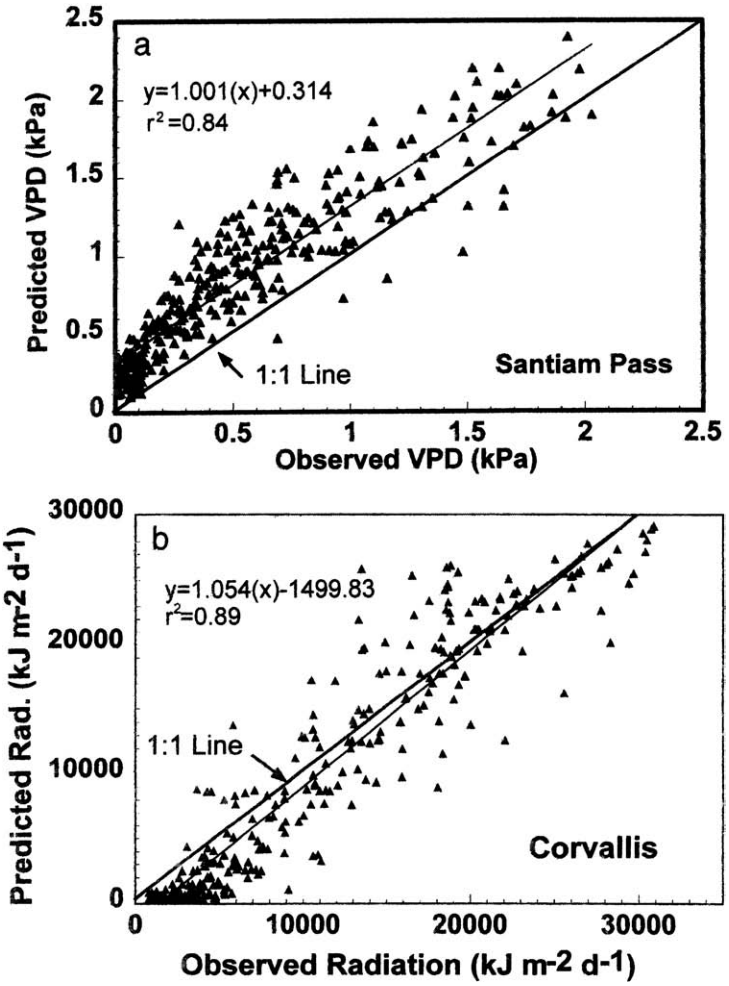

FIGURE 7.5. Comparison of MT-CLIM estimates of daily incident solar radiation and vapor pressure deficit for two sites on the Oregon transect. Most weather stations report only daily temperature and precipitation, so MT-CLIM provides estimates of solar radiation and humidity conditions that may otherwise be unobtainable. (From Glassy and Running, 1994.)

the diurnal temperature range serves as the basis for calculating the clarity (*transmittance*) of the atmosphere. The general principle expressed here is that the range of diurnal temperature is highest on clear days, and that cloudy and/or hazy days result in much smaller temperature ranges. Atmospheric transmittance is a general measure of the attenuation of solar radiation caused by clouds, haze, and aerosols. Elevation determines the atmospheric path length, so is a strong determinant of clear sky transmissivity.

MT-CLIM begins with an optical transmissivity set at sea level of 0.65, then increases clear sky transmissivity by $0.08\,km^{-1}$ of elevation. Next, the diurnal temperature range,

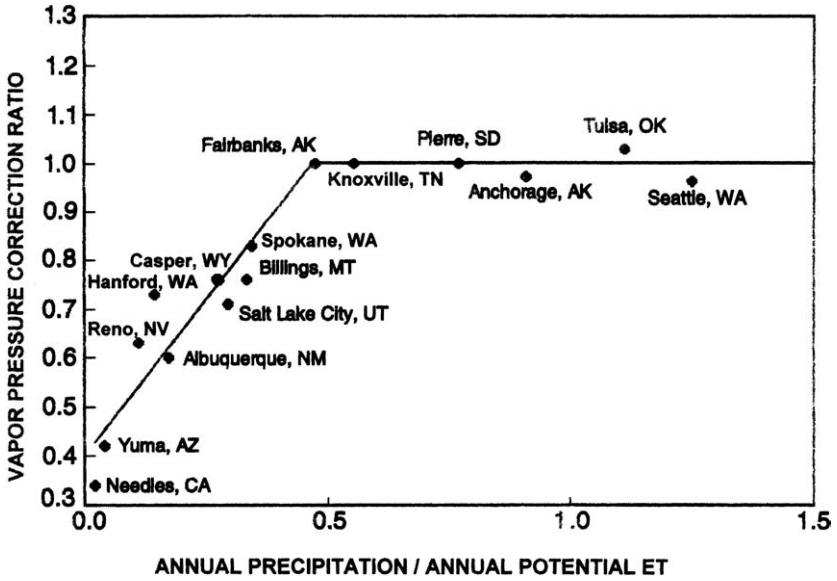

FIGURE 7.6. The MT-CLIM model assumes that measured night minimum temperature equals the daily dew point, which is then used to compute vapor pressure deficit. Kimball *et al.* (1997b) found this T_{min}-dew point assumption to be valid in climates where annual precipitation reaches at least 50% of annual potential evapotranspiration (ET). In drier climates, where minimum temperatures may not reach the dew point, the ratio annual precipitation/annual potential ET provided an accurate means of estimating vapor pressure at weather stations scattered across the United States. (After Kimball *et al*., 1997b.)

ΔT, is calculated from the daily maximum temperature and minimum temperature (°C). The relationship between diurnal temperature amplitude and atmospheric transmittance is then calculated using an exponential formulation that defines an asymptotic relationship of transmissivity with progressively larger variation in diurnal air temperature. On average, with completely clear skies, a 20°C diurnal temperature range is observed, with certain seasonal and regional modifications. Multiplying potential (top of atmosphere) radiation by the atmospheric transmissivity gives an estimate of daily solar radiation at the surface. These MT-CLIM estimates of daily solar radiation have been tested repeatedly against measured incident solar radiation, and correlations consistently show $r^2 > 0.85$ (Fig. 7.5; Glassy and Running, 1994; Running *et al*., 1987).

B. Topographic Extrapolations

The previous sections have illustrated how to compute the necessary suite of daily meteorological variables from limited weather data at a single station. Now we must extend the approach to predict meteorological variables across the landscape. MT-CLIM was designed with the assumption that daily weather data would be primarily available from standard stations usually located in valley bottoms near airports. To represent the microclimates of adjacent, more complex topography requires spatially extrapolating these valley bottom conditions to higher elevations and to various combinations of slope and aspect. A set of

procedures now exist to present the spatial variability of solar radiation, air temperature, and precipitation in complex terrain.

1. Solar Radiation

The most obvious microclimatic effect of topography, especially at high latitudes, is on incident solar radiation. Many studies have shown how extreme microclimate and forest responses differ on north and south facing slopes (Lee and Sypolt, 1974; Tesch, 1981b; Running, 1984b). Fortunately, the solar geometry calculations used in MT-CLIM from Garnier and Ohmura (1968) and Swift (1976) provide a means for computing the incident radiation to any combination of slope/aspects each day of the year (Fig. 7.7). One obvious application of solar geometry is to predict the easily observed differences in the disappearance of snow from different aspects. In the mountains of Montana (44°–47°N latitude), it is common to see south facing slopes melt free of snow 1–2 months earlier than adjacent north slopes at the same elevation (Wigmosta *et al.*, 1994).

2. Air Temperature

Climatologists have long measured the direct change in average air temperature associated with decreasing atmospheric pressure at higher elevations (Baker, 1944; Barry, 1992). These elevational *lapse rates* usually average −7° to −9°C km^{-1}, although considerable day-to-day variation occurs in response to air mass movement and precipitation (Fig. 7.8). The first step in MT-CLIM for extrapolating a valley bottom temperature to a mountain hill slope is to subtract an average lapse rate based on the elevational difference between the two points.

The next step of computing aspect-related temperature differences relies on the computed solar radiation differences as described above. Hill slope air temperatures, however, are also influenced by wind patterns, surface vegetation, and energy budgets. The MT-CLIM program uses empirical weighting coefficients to add or subtract air temperature from an observed base station temperature as a ratio of the solar radiation received on a slope to that received on a flat surface. Thus, a south slope in the northern hemisphere which receives more solar radiation will be 1°–2°C higher, whereas a north facing slope will be 1°–2°C lower than a flat surface. More sophisticated computations of these microclimate differences are available, but they require much more computer time and demand more data than available to most resource managers (Pielke *et al.*, 1992).

3. Precipitation

Precipitation estimates in mountainous terrain must primarily be able to represent the orographic influences of the topography on the prevailing storm track. In the western United States, annual precipitation in the valley bottoms can be one-tenth that recorded in the surrounding mountains. Daly *et al.* (1994) used statistical analysis of station data embedded in a digital terrain model to compute regional precipitation. Thornton and Running (1996) and Thornton *et al.* (1997) developed DAYMET, which embeds the original MT-CLIM in a digital topography to allow weighted interpolation of data between many stations (see Plate 3).

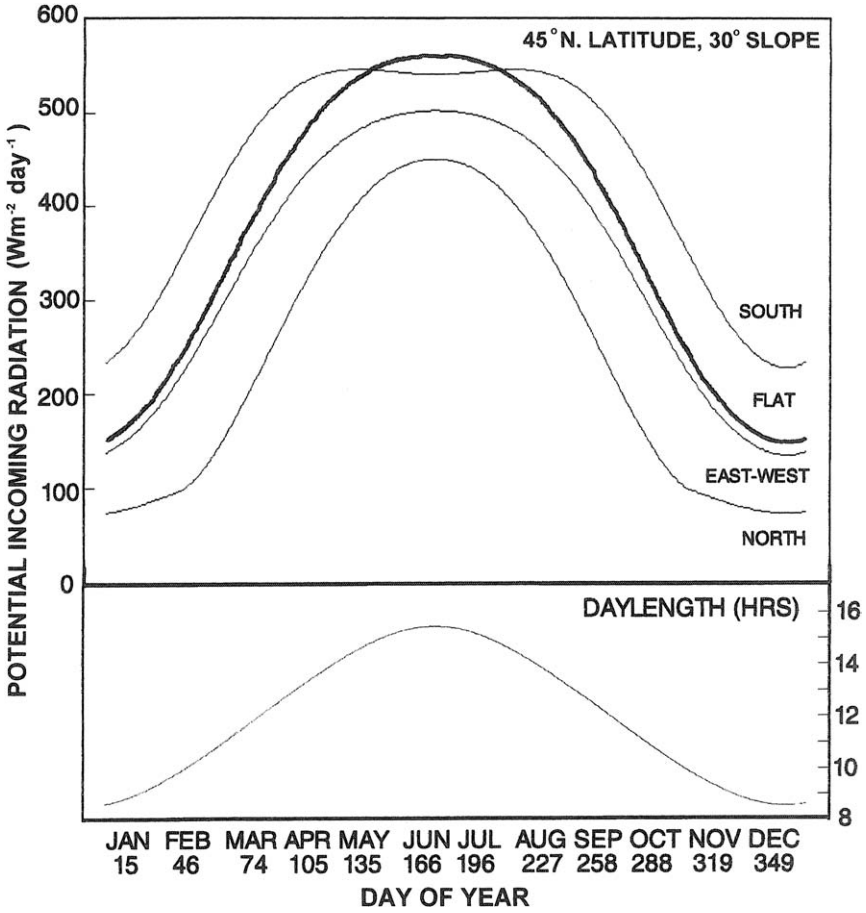

FIGURE 7.7. Comparison of incident potential (or cloud-free) solar radiation with aspect and season computed by MT-CLIM. This example is for a 30° slope at 45° N latitude, but the model can compute any slope/aspect/latitude combination. Note that for this latitude and slope the relative differences in radiation loads on different aspects are highest outside the growing season. In fact, north facing aspects may receive no direct radiation for almost 3 months in midwinter. Differences in annual radiation loads are the primary driving force associated with aspect-related differences in vegetation found throughout arid lands at mid- to high latitudes. Differences in radiation loads on slopes of varying aspect are much less in cloudy climates and at lower, tropical latitudes.

4. Wind

Wind is an important factor in the energy and water budgets of canopies, often expressed through an aerodynamic resistance term (Fig. 2.5). It has been difficult, however, to apply climatological principles that can predict wind speed from our limited selection of microclimatic variables. Unless direct measurements of wind are available, a moderate wind speed equivalent to a light breeze, around 2 m sec^{-1}, is often assumed. The error involved in this assumption is small for most forests, which are well coupled to the atmosphere, but becomes larger with vegetation of shorter stature (Chapter 2).

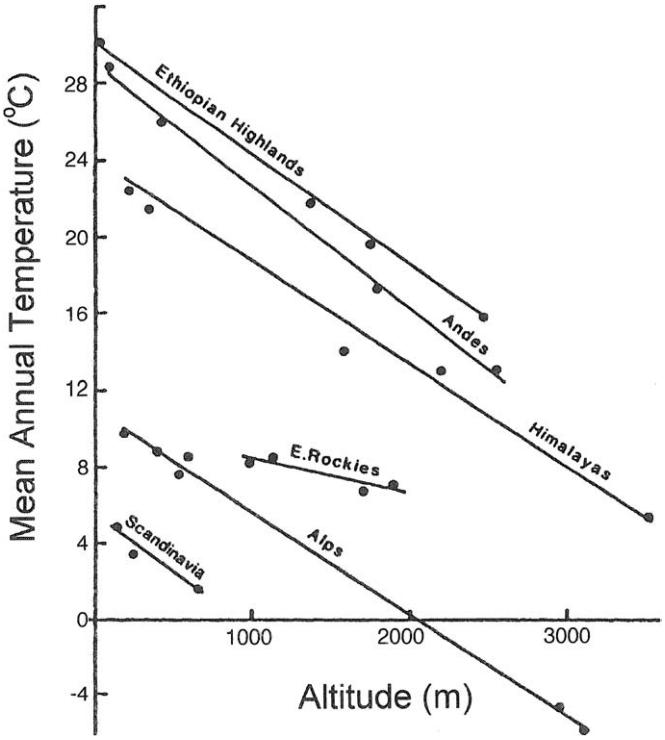

FIGURE 7.8. Observed elevational lapse rates (decrease in air temperature produced by decreased barometric pressure with altitude) for mountain ranges all over the world. (From Friend and Woodward, 1990.)

IV. DESCRIBING THE ECOSYSTEM

Forested landscapes have commonly been described by defining vegetation units or by calculating the commercial potential to grow trees. Neither approach provides a quantitative measure of system attributes important for ecosystem analysis. Vegetation classifications incorporate knowledge about species assemblages but lack information on biophysical attributes. Commercial assessments of standing volume are insufficient by themselves to derive estimates of leaf area or autotrophic respiration. Moreover, both types of information are generally dependent on infrequent ground sampling on relatively small areas. For consistent and continuous monitoring of landscape properties, some broader, more frequent sampling is required, and this leads us into the field of remote sensing.

A. Principles of Remote Sensing

Any serious quantitative study of a landscape must begin with some type of remote sensing; there is no other way to obtain consistent measurements across large areas, Remote sensing originated with aerial photographs taken by cameras from airplanes and balloons, technology still used today for certain applications. Photographs, however, are

difficult to compare over time as lighting conditions and film quality vary. An array of new sensors produce digital images that are preferred because the raw data can be manipulated, processed, and stored in a computer. As with cameras, sensors can be mounted on aircraft, balloons, truck booms, or satellites. The important distinction is that digital data provide a superior format with greater spectral and radiometric accuracy required for comparative analyses of landscapes (Lillesand and Kiefer, 1994; Jensen, 1996).

With the launch of the U.S. Landsat 1 series of satellites in 1972, scientists first tried to repeat the same forest inventory and vegetation classifications that were possible from ground surveys. They found, however, that the satellite-based surveys could provide adequate predictions only when correlated with specific ground-based data. Computer-assisted classification of spectral reflectance data were of two types: *supervised*, where spectral signatures were assigned to known landscape units, and *unsupervised*, where the landscape was distinguished by spectral differences without any previous attempt to recognize the composition of the units (Lillesand and Kiefer, 1994; Jensen, 1996). The classification techniques were applied to map stand density, timber volume, and forest types. All of these techniques, however, were derived from statistical associations that were not biophysically based, and thus they produce only local correlations that cannot be transferred to new areas. To build remote sensing tools of general utility for landscape analysis, one must match the capabilities of the technology with more fundamental ecological attributes. Landscape variables such as canopy size and structure, soil color, and surface temperature can be remotely sensed. Other variables such as tree gas emissions, soil chemistry, and rooting depth do not directly alter properties of the electromagnetic spectrum; they may be inferred but cannot be measured.

Forests are among the most challenging types of vegetation to decipher with remote sensing (Peterson and Running, 1989). Trees are present in a wide range of sizes, shapes, and colors. Tree canopies can range in height from 1 to 100 m. Broadleaf trees exhibit marked seasonal variation in canopy display, while evergreen trees show little detectable seasonal variation. Mixtures of evergreen and deciduous trees are common. The ground surface below trees often supports other vegetation such as grasses with different reflectance characteristics, which may alter the average reflectance properties of the ecosystem. Forests are located in regions with complex topography, and occur at high latitudes, factors that induce shadowing. Consequently, only a small number of remotely sensed properties are available to assess the state of forest ecosystems in a dependable manner (Verbyla, 1995).

An important distinction is made in remote sensing between the *radiances* that are measured by the sensor and the *reflectances*, which represent the fraction of incoming radiation in a particular spectral region that is emitted or reflected from the surface (Fig. 7.9). This seemingly subtle distinction is most easily understood by considering an evergreen forest imaged every day by a satellite sensor for several weeks. While no property of the forest canopy may change over this short period, and hence the absolute reflectance would not change, the radiances measured from a satellite may change considerably because of variability in the clarity of the atmosphere, view angle of the sensor, and intensity of solar illumination. To discern real changes in landscape properties, procedures to correct for or normalize these sources of variability in radiance must be applied (Verbyla, 1995).

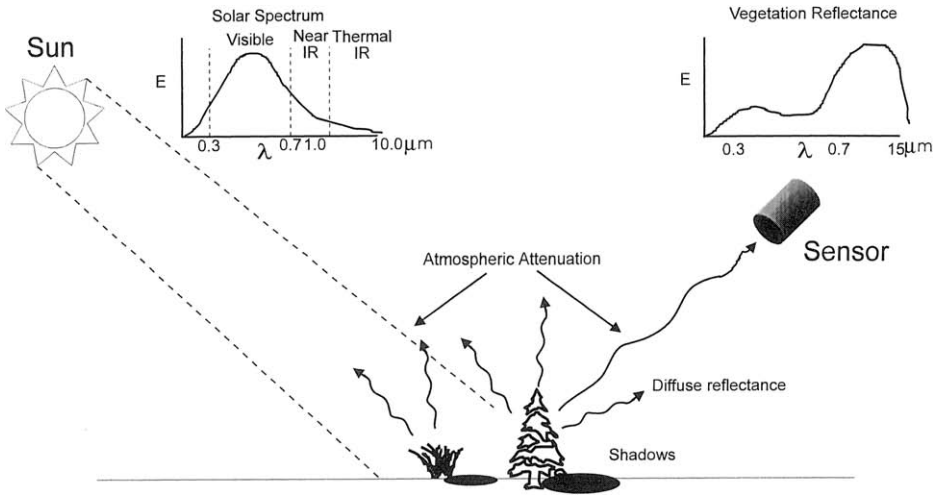

FIGURE 7.9. Important principles of the geometric relationships among the source, target, and sensor that apply to all terrestrial remote sensing. The sun's energy is attenuated by the atmosphere in all directions, but to varying degrees dependent on the wavelength. The angle of solar illumination and view angle of the sensor determine how much sunlit or shaded surface the sensor observes. Remote sensing sensors typically look straight down, from a nadir view, but advanced sensors analyze reflectance differences from various view angles to improve estimates of canopy structure.

In evaluating the potential application of remote sensing it is useful to consider four dimensions: spatial, spectral, temporal, and directional. Each of these dimensions offers special advantages in interpreting landscapes, which we will clarify in the following discussion.

1. Spatial Resolution

To someone unfamiliar with remote sensing, it would seem that a landscape viewed at highest possible resolution would always be the preferred option. Early Landsat satellites provided a square picture element (*pixel*) about 80 m on a side; the Landsat TM sensor now provides 30 m resolution, and the French SPOT satellite carries a sensor that can resolve detail to 10 m resolution. The volume of data, we must recognize, increases geometrically with decreasing pixel size. A first 1-km resolution view of Earth (1.4×10^8 pixels) from the National Oceanic and Atmospheric Administration (NOAA) Advanced Very High Resolution Radiometer (AVHRR) sensor has only relatively recently been attempted (Eidenshink and Foundeen, 1994). A global Landsat data set does not exist, simply because the data volume and number of scenes required to produce a cloud-free image (150 billion pixels) is too great. Thus, very high spatial resolution is desirable primarily for local studies.

A second problem associated with high spatial resolution data is that variability increases as additional small details become visible. For example, a seemingly smooth desktop viewed under a microscope reveals variation in wood structure not visible at the more coarse resolution of the naked eye. For broad studies with a rather simple goal, such as

quantifying the national area in forest cover, it is efficient to have the sensor provide a spatially averaged representation at 1 km resolution or larger. Quantifying the same forest cover for a landscape that has been heavily logged in 10-ha patches, however, would require a sensor with 30 m resolution. Even at 10 m spatial resolution, the canopy of individual trees cannot be resolved. Aircraft-mounted sensors, on the other hand, are of particular value for local studies because virtually any level of spatial detail is obtainable from <1 to $>1000\,m^2$.

With these cautions in mind, any regional ecology project that applies remote sensing must consider the size and heterogeneity of the area being studied, as well as the specific objectives of the study. In general, one should choose a spatial scale with a pixel size as large as possible to minimize the cost of acquiring and processing data. We caution readers that geography literature typically uses the term "scale" in the opposite sense of ecologists. "Large scale" to a geographer means that ground features are represented at a larger, more detailed size, whereas to an ecologist the term means a larger area is being represented, resulting in ground features being represented in less detail.

2. Spectral Resolution

Vegetation is typically analyzed with spectral bands in the visible red (Red) and near-infrared (NIR) range (Asrar, 1989). Current satellites carry sensors that measure reflectances between about 0.4 and 10 μm with three to four channels that are selected to avoid water absorption wavelengths (Fig. 7.10). The most common reflectance indices associated with vegetation are the Simple Ratio (SR) of NIR to Red reflectance and the normalized form of those two bands, called the Normalized Difference Vegetation Index or NDVI:

$$SR = NIR/Red \tag{7.1a}$$

$$NDVI = (NIR - Red)/(NIR + Red). \tag{7.1b}$$

The particular wavelengths selected differ among sensors, and many other spectral ratios have been proposed for various purposes. All make use of the general remote sensing principle that plant canopies absorb much of the radiation in the visible wavelengths and reflect more in the infrared. The predominant wavelengths of interest in the infrared are 0.7–0.9 μm, often called the near-infrared. Representing these radiances as a ratio minimizes atmospheric influences and also differences in sensor geometry (sun–earth–sensor angles) without greatly complicating data processing (Lillesand and Kiefer, 1994).

New sensors have been built and tested from aircraft that provide continuous spectral coverage from 0.4 to 2.5 μm in 200–300 channels, almost equivalent to laboratory spectrometers (Curran, 1994). Spectral studies conducted in laboratories and greenhouses demonstrate that leaf lignin, chlorophyll, and nitrogen concentrations, as well as water content, may be assessed nondestructively with high spectral resolution sensors (Gamon *et al*., 1992; Field *et al*., 1994). Increases in each of these leaf constituents tend to enhance near-infrared reflectances and result in raising the SR, NDVI, and other related spectral combinations (Matson *et al*., 1994; Yoder and Waring, 1994). Carter (1994) expanded the approach by interpreting leaf reflectance changes as indicators of plant responses to environmental and chemical stresses. Because of the complex geometry of canopies, however, and the necessity for sophisticated atmospheric corrections, it has been difficult to extend

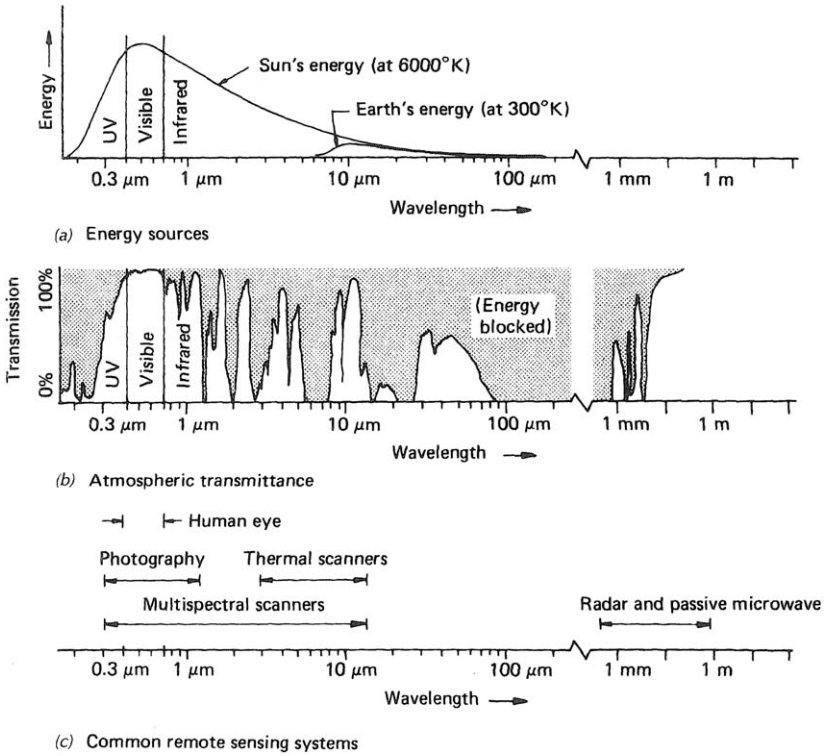

FIGURE 7.10. Spectral characteristics of solar and terrestrial electromagnetic energy. Wavelengths at which water vapor, aerosols, and greenhouse gases strongly absorb are identified. The spectral channels common to a range of remote sensing systems have been chosen to avoid atmospheric absorption regions and to emphasize regions of reflectance valuable in assessing land surface properties. (After T. M. Lillesand and R. W. Kiefer, *Remote Sensing and Image Interpretation*, 3rd Edition, Copyright © 1994 by John Wiley & Sons, Inc. Reprinted by permission of John Wiley & Sons, Inc.)

fine-resolution spectral analyses to general field conditions (Zagolski *et al.*, 1996; Martin and Aber, 1997).

Some of the solar energy incident on a forest is absorbed, heats the surface, and is then emitted as thermal energy in wavelengths from 8 to 12 μm, as discussed in Chapter 2. Current satellite sensors usually contain one or two channels in the thermal region, and this emitted radiation provides a basis for calculating a radiometric surface temperature (Price, 1989). There are many ecological applications for landscape temperature maps, but one must recognize that these radiometric surface temperatures can be much different than the near-surface air temperatures recorded at weather stations. The largest differences, which can reach temperatures of 30°C above that of ambient air, occur on bare, dry soils under high solar radiation (Fig. 7.11; Norman *et al*., 1995).

Vegetated surfaces also emit radiation in wavelengths from 1 mm to 150 cm, the microwave and radar region. Passive microwave sensors measure the weak naturally emitted radiation from surfaces in these wavelengths (Engman and Chauhan, 1995). Active radar

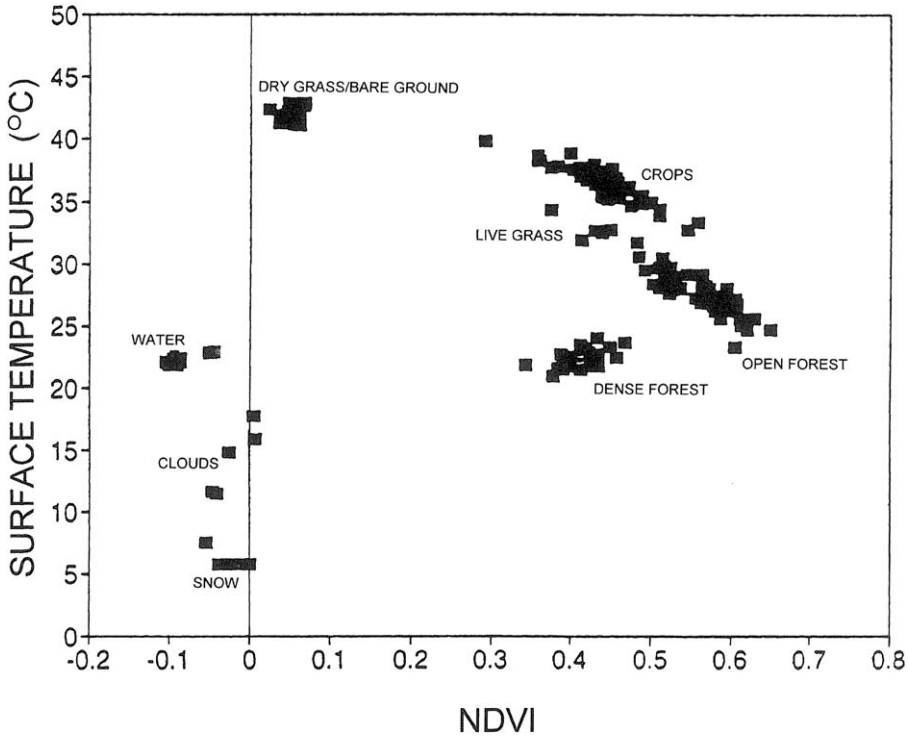

FIGURE 7.11. Variation in radiometric surface temperature observed by AVHRR for 14 July 1987, 1430 hr local time, for a complex 106,000-km^2 region with farmland, rangeland, and forestland in Montana (Nemani and Running, 1989b; Nemani *et al*., 1993a). The 40°C range in surface temperatures observed across the region result from varying albedo and energy partitioning to latent or sensible heat, and aerodynamic coupling of the vegetation (see Chapter 2). Surfaces with higher vegetation cover and LAI (as defined by the NDVI) exhibit surface temperatures below 25°C which approaches ambient surface air temperatures. Nearby, recently cleared areas exhibit temperatures above 45°C.

sensors emit a pulse of energy and analyze the return signal (Dobson *et al*., 1995). A key feature of passive microwave and radar is their ability to receive signals through clouds, haze, smoke, or at night when optical sensors are useless (Waring *at al*., 1995b). Radar data, however, are difficult to interpret because microwaves are scattered and bounce off surfaces multiple times before returning to the sensor. Processing is particularly complicated when look angles and polarization fields are varied to obtain additional information (Lillesand and Kiefer, 1994). Despite these difficulties, imaging radar has special merit in discerning flooded, frozen, and drought-stressed forests, and for research in perennially cloudy or solar-limited regions at high latitudes.

3. Temporal Resolution

The highest temporal coverage currently available with a satellite is every 30 minutes, provided by the Geostationary Operational Environmental Satellites (GOES) weather sat-

ellites. To remain geostationary, these satellites circle 36,000 km above the equator in tne same direction and speed as Earth rotates. Because of the high altitude orbit these geostationary satellites offer limited spatial resolution and at present also are restricted in spectral coverage and radiometric accuracy. The AVHRR sensor, which is primarily used for weather forecasting, provides daily coverage, but on some orbits must look at extreme angles as much as 55° from nadir. AVHRR experts prefer to use data from <30° look angles to minimize atmospheric path length effects and pixel elongation, which means that acceptable data may be available at 3- to 4-day intervals depending on latitude (Goward *et al*., 1991). Sensors that provide high spatial detail such as Landsat and SPOT have 16- and 26-day repeat cycles because their lower orbits produce a narrower swath across Earth's surface.

Clearly, there is a choice that must be made between acquiring greater spatial detail and temporal coverage. This choice must be made in reference to the scientific objective and the type of satellite-derived data available. Also, the daily overpass time must be considered because the likelihood of encountering cloudy or hazy conditions limits the acquisition of optical data. The day-time AVHRR sensor is synchronized to pass over all sites at mid-afternoon (1430 solar time), while Landsat acquires data at 0945. Controls in some satellites are inadequate to prevent a drift in orbits which results in a progressive shift in overpass times. The Earth Observing System (EOS), launched since 2000, will carry the Moderate Resolution Imaging Spectroradiometer (MODIS) sensor in a similar orbit to AVHRR, with 36 spectral channels and spatial resolution of 250 m, 500 m, and 1 km. By employing two satellite platforms, MODIS collects data at both 1030 and 1330 (Running *et al*., 1994).

Because of the temporal constraints reviewed above, Landsat and SPOT sensors have shown the most general utility for local to regional analyses. AVHRR has served predominantly for assessing seasonal variation in ecosystem activity at regional to global scales. In combination, one can attain high spatial detail from Landsat or SPOT, then follow the temporal activity of landscapes with AVHRR or MODIS.

4. Directional Options

A new dimension of remote sensing has been gained by allowing sensors to look at the surface from multiple angles (Irons *et al*., 1991; Ranson *et al*., 1994). From these off-nadir perspectives dramatic differences in reflectances are observed. For example, visualize the difference of viewing a tree from above on its sunlit side, where the foliage is entirely illuminated, and viewing the same tree from the shaded side where much of the canopy is in shadow (Hall *et al*., 1995).

Regardless of what combination of the four remote sensing properties are employed to distinguish surface features, much training and specialized equipment are required to process the raw data (Lillesand and Kiefer, 1994; Jensen, 1996; Ryerson, 1996). Fortunately, most image processing programs now run on personal computers. In addition, new programs like NASA's Earth Observing System should further simplify analyses by providing selected sets of fully processed data in a georeferenced form (Running *et al*., 1994).

B. Remotely Sensed Landscape Attributes

1. Albedo, Land Cover, and Snow

As discussed in Chapter 2, albedo quantifies the fraction of short-wave radiation reflected from the land surface. Albedo affects the energy balance and is thus an important variable for all climate models, as will be discussed in Chapter 9. Albedo can be defined for specific spectral regions (a spectral albedo), but it most often includes the total short-wave reflectance. The total short-wave reflectance provides an excellent means of discriminating between water, bare land, snow, ice, and vegetation on a seasonal basis using data acquired from various satellites (Chapter 9). Because water absorbs short-wave radiation almost completely, surface albedo is particularly valuable for distinguishing the distribution of floodwaters. At the other extreme, snow has a high albedo, so the presence of snow cover and the timing of its disappearance can be monitored from satellites, assuming cloud cover is not prevalent.

2. Satellite-Derived Surface Meteorology

Meteorological satellites can provide an alternative means of obtaining weather data to drive ecosystem models. Meteorological satellites have either continuous or daily global coverage, but they are often limited in their spatial resolution as a result of the high altitude of their orbits. Regular archiving of these data is often required at even coarser resolution. As yet, procedures for processing and distributing these derived data sets are not standardized. Estimates of surface meteorology are also somewhat restricted by cloud cover, although the amount of cloud cover can he monitored and conversions made to predict incoming solar radiation and diurnal variations in temperature. Goward *et al*. (1994) estimated the monthly integrated incident solar radiation across the Oregon transect with high accuracy from ultraviolet reflectance data collected with the Nimbus-7 TOMS (Total Ozone Mapping Spectrometer) (Fig. 7.12a). Annual global incident radiation was mapped by Dye and Shibasaki (1995) using the same methodology. The GOES geostationary satellites are typically used to estimate daily PAR, because cloud cover and aerosol calculations can be done every half hour throughout the day. Daily estimates of incident solar radiation typically agree well with ground observations, with $r^2 > 0.95$ (Frouin and Pinker, 1995; Pinker *et al*., 1995).

Meteorological satellites also provide good estimates of surface temperatures as illustrated from a summertime mid-afternoon sampling acquired over 106,000 km^2 (Fig. 7.11). Variation across the scene illustrates the effects of variable aerodynamic mixing and evapotranspiration from surfaces with differing cover of vegetation. The coolest surfaces (22°–25°C) represent dense forests or lakes, and closely correspond with measured air temperatures. Dry grass and bare ground were >40°C. Goward *et al*. (1994) demonstrated

---

FIGURE 7.12. Satellite sensors provide an alternative to extrapolation of surface weather observations as Goward *et al*. (1994) demonstrated across the Oregon transect (see Fig. 1.4). (a) Comparison of monthly integrated PAR derived from daily observations made with the TOMS sensor, (b) air temperatures estimated with AVHRR, and (c) estimated vapor pressure deficits from a combination of optical and thermal sensors, all compared against ground observations. (From Goward *et al*., 1994.)

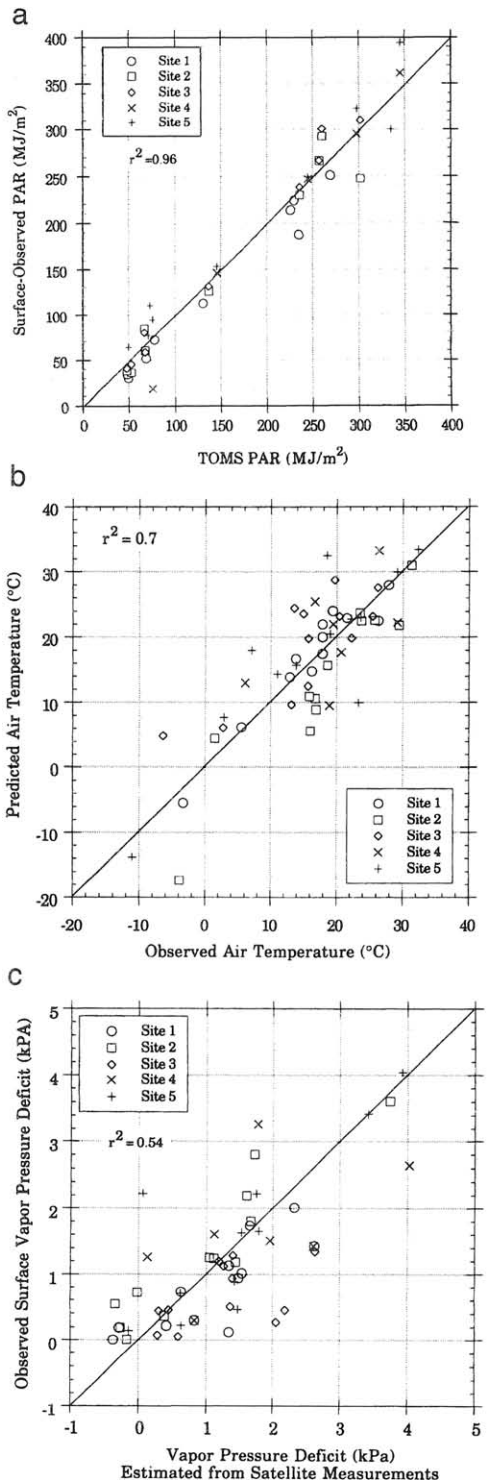
a
Site 1
Site 2
Site 3
Site 4
Site 5
r^2=0.96
Surface-Observed PAR (MJ/m^2)
TOMS PAR (MJ/m^2)
b
r^2 = 0.7
Predicted Air Temperature (°C)
Observed Air Temperature (°C)
c
r^2 = 0.54
Observed Surface Vapor Pressure Deficit (kPA)
Vapor Pressure Deficit (kPa)
Estimated from Satellite Measurements

that it is possible to estimate ambient air temperatures even on a range of lightly vegetated surfaces by extrapolating the thermal infrared surface temperatures to conditions equivalent to full canopy closure (Fig. 7.12b). Norman *et al*. (1995) reviewed a variety of methods for computing surface temperatures with satellite thermal–infrared data.

Using satellite data to estimate surface humidity is problematic because water vapor in the atmospheric profile is a major cause of attenuated reflectances. One possible approach is to compute a surface temperature during the night overpass of a polar orbiting satellite (12 hr opposite the daytime pass) and apply the T_{min} versus T_{dew} relationship. However, image navigation of nighttime scenes is difficult, so only approximate locations are possible. Another method, called the split-window approach, analyzes the variable response of two thermal channels, one sensitive to water vapor and one not. Goward *et al*. (1994) applied the split-window approach to estimate vapor pressure deficits during satellite overpass times across the Oregon transect (Fig. 7.12c).

Satellite-based estimates of surface rainfall are best accomplished by microwave sensors, although these sensors have only 15 km spatial resolution. Efforts to use visible/NIR sensors at 1 km correlate cloud cover with rainfall, so have been only partially successful (Petty, 1995). Estimating daily rainfall over small areas is particularly difficult, but monthly regional rainfall can be fairly accurately determined because the random distribution of small thundershowers is averaged out.

These satellite-based techniques provide the most complete spatial representation of surface meteorology possible, and they are particularly valuable for quantifying meteorological variability in complex terrain and over variable cover of vegetation. Unfortunately, these surface meteorology products are not archived routinely and often are available only at a rather coarse spatial resolution.

3. Surface Resistance/Wetness

When NDVI and surface temperature are plotted together in a two-dimensional graph, a predictable pattern emerges. After screening out pixels of clouds and snow, we see that forests have the coolest temperatures, and bare surfaces the warmest (Fig. 7.11). If this analysis is repeated through the growing season, a trend emerges. In the spring, the ground is wet, so bare soil surface temperatures are relatively low and differ little from forest canopy temperatures. As summer progresses and the landscape dries out, bare soil and dry grasses heat up faster than forests, and so the trend line between $T_{surface}$ and NDVI becomes steeper. Nemani and Running (1989b) related the change in $T_{surface}$ versus NDVI to a simulated canopy resistance from FOREST-BGC for a Montana forest landscape that shows severe summer drought (Fig. 7.13). We call this analysis a *surface resistance*, because it operates as a landscape-level measure of canopy resistances as well as that associated with evaporation from the ground. Effectively, this surface resistance is a simple aggregate measure of the landscape Bowen ratio ($H/\lambda E$), where as incident radiation is progressively dissipated to sensible, rather than latent heat, surface temperatures increase. This AVHRR-defined surface resistance is particularly effective because the satellite overpass time is roughly 1430 local time, and the date selected from each biweekly set of daily data represents the clearest and sunniest day observed during the sampling period.

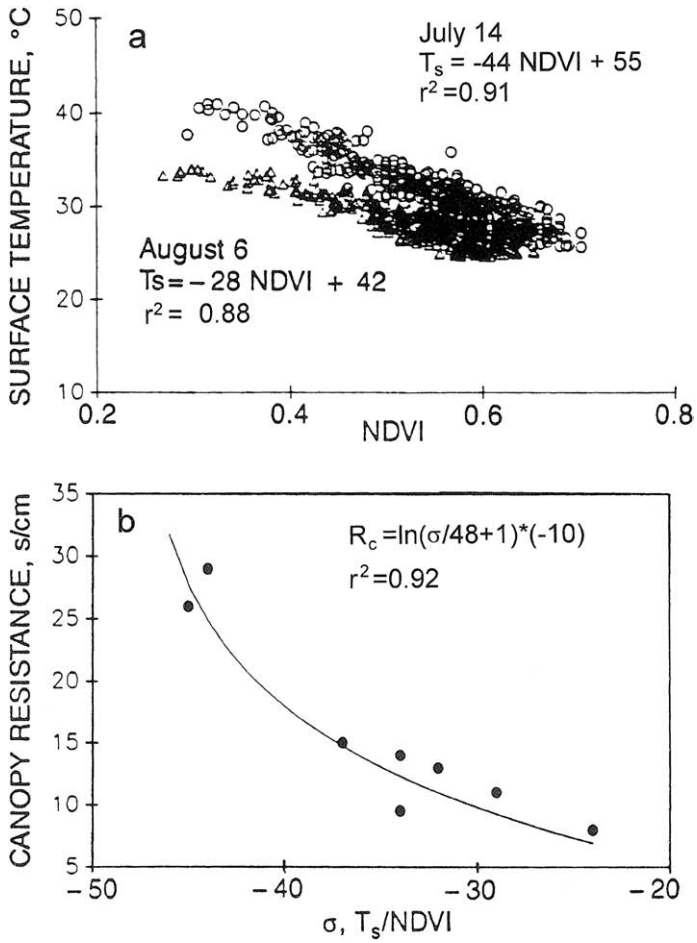

FIGURE 7.13. (a) As the land surface dries, exchange of latent energy declines, and the slope of the scatter of points in Fig. 7.11 becomes steeper as sensible heat exchange and surface temperatures (T_s) increase. (b) This change in the T_s/NDVI scattergram was expressed as a regional surface resistance to evapotranspiration by Nemani and Running (1989b) and Nemani *et al*. (1993a). The change in slope of T_s/NDVI computed for 8 clear days during the summer of 1987 was closely related to canopy resistance simulated by FOREST-BGC.

4. Leaf Area Index and Fraction of Light Absorbed by Canopy

Estimation of LAI across a landscape is essential for regional ecosystem analyses. Because the seasonal variation in LAI is important, considerable effort has been expended to develop nondestructive optical methods to estimate this variable. Initially a simple Beer's law inversion with a fixed extinction coefficient was applied to estimate LAI by measuring the attenuation of PAR through the canopy (Chapter 2; Pierce and Running, 1988). This simple analysis works well for many broadleaf canopies (Burton *et al.*, 1991; Wang *et al*., 1992a), but for many evergreen species more complicated procedures are required to

account for deviations from Beer's law caused by shadows and clumping of needles (Gower and Norman, 1991; Lang, 1991; Nel and Wessman, 1993; Smith *et al*., 1993; Fassnacht *et al.*, 1994; Stenberg, 1996). With accurate ground estimates of LAI now available, attempts to remotely sense this variable have greatly increased.

Canopy radiation models tested on a wide variety of forests consistently predict a curvilinear relationship between LAI and a spectral vegetation simple ratio or its derivative NDVI (Myneni *et al*., 1997a) (Fig. 7.14a). This results in NDVI not being an accurate predictor of LAI much above values of 4. Spanner *et al*. (1990, 1994) documented the curvilinear trend predicted by models across the broad range of LAI available on the Oregon transect (Fig. 7.14b). Chen and Cihlar (1996) used Landsat TM to test both the NDVI and SR for computing LAI of boreal pine and spruce stands. The highest correlations between NDVI and SR to overstory LAI were obtained with Landsat data from the springtime before understory plants produced leaves. Soil and understory plants produce a background that can be spectrally brighter than the forest canopies, and cause erroneous satellite estimates of overstory LAI. Nemani *et al.* (1993c) obtained increased precision in estimating LAI in forest stands across Montana when a mid-infrared band was added to the analysis. They concluded that with AVHRR 1-km data, part of the sensitivity of the NDVI is to canopy closure and masking of the soil surface reflectance. Pierce *et al*. (1993) also quantified LAI of *Eucalyptus* forests with AVHRR-derived NDVI.

If a landscape is being defined for a comprehensive biogeochemical simulation such as RHESSys (Fig. 7.2), LAI may be the preferred canopy variable because it is required for estimating so many process rates, from canopy gas exchange to nutrient return in litterfall (Bonan, 1993). If the objective is narrowed to obtain estimates of NPP only, then a Light Use Efficiency model, as described in Chapter 3, can be initialized from a measure of the fraction of PAR absorbed, or FPAR. LAI and FPAR are closely related: LAI defines the canopy structure directly, whereas FPAR defines the radiometric result of light attenuating through the canopy with a given LAI (Sellers *et al*., 1992a). Equation (2.7) can be solved by either entering LAI and calculating FPAR [I in Equation (2.7)], or entering FPAR and solving for LAI. Goward *et al.* (1994) predicted FPAR for the Oregon transect sites from AVHRR-derived NDVI measurements and found generally good agreement with ground-based estimates (Fig. 7.15). Prince and Goward (1995) extended the FPAR estimates from NDVI to compute NPP for all terrestrial ecosystems with their Global Production Efficiency Model (GLO-PEM).

5. Biomass, Structure, and Density

The ability of remote sensing techniques to quantify forest stand structure has steadily improved from aerial photography through Landsat, SPOT, and now advanced radar and multidirectional sensors (Peterson and Running, 1989; Lillesand and Kiefer, 1994; Sample,

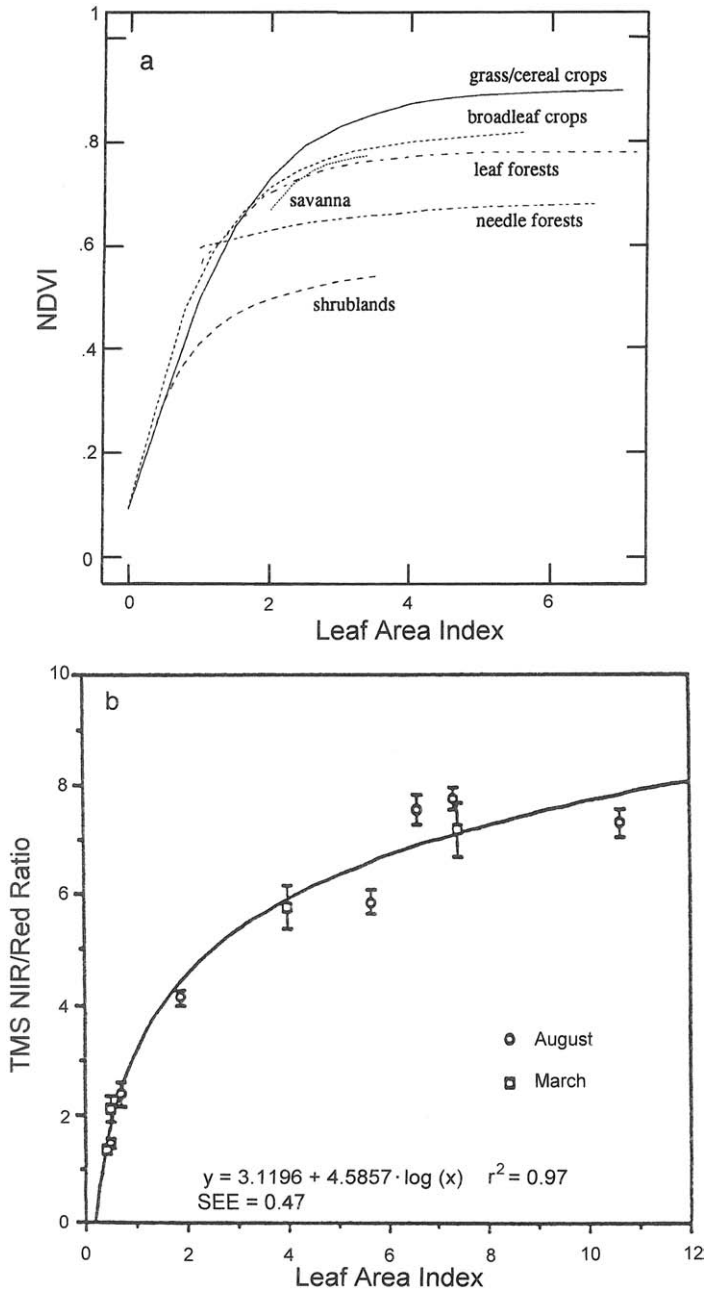

FIGURE 7.14. Calculation of LAI from satellite NDVI data (a) as predicted by a theoretical canopy radiative transfer model for various biome types by Myneni *et al*. (1997a) and (b) as measured for coniferous forests across the Oregon transect by Spanner *et al*. (1994). (From Mynemi *et al*., "Algorithm for the estimation of global landcover, LAI, and FPAR based on radiative transfer models," *IEEE Transactions in Geoscience and Remote Sensing*, © 1997 IEEE; and from Spanner *et al*., 1994.)

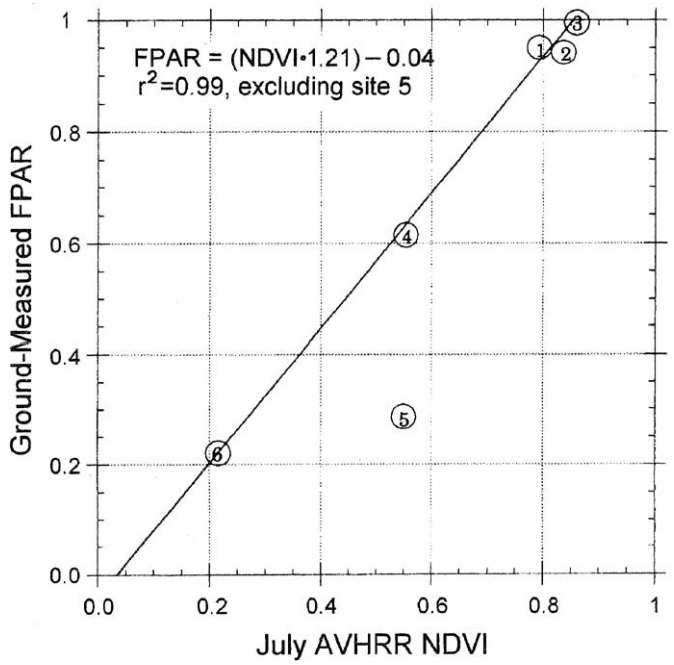

FIGURE 7.15. Fraction of PAR absorbed (FPAR) computed from NDVI for coniferous forest canopies of the Oregon transect (Goward *et al*., 1994). Canopy radiative transfer theory predicts NDVI to be more linearly related to FPAR (a radiometric variable) than to the structural variable LAI. FPAR is used primarily for computation of NPP with Light Use Efficiency models (see Chapter 3), whereas LAI is required in more sophisticated process models such as FOREST-BGC and RHESSys. The regression line was defined by excluding plot number 5 on which ground measurements were made in a recently thinned ponderosa pine stand that differed from the surrounding 1-km^2 area sampled by the satellite sensor. (From Goward *et al*., 1994.)

1994; Verbyla, 1995). A multisensor approach is sometimes valuable to provide more complete spatial and temporal coverage. Iverson *et al*. (1994) used both AVHRR and TM data to map forest cover of a 13-state region of the midwestern United States. They first analyzed TM scenes to calibrate the larger scale AVHRR imagery and then extended the classification to the broader region. Correlations with ground-based forest cover estimates averaged $r^2 = 0.8$. Cohen and Spies (1992) combined SPOT and TM data to estimate forest structure of conifer forests in the Pacific Northwest. They concluded that tree size and overstory density were well correlated with a number of spectral indices and obtained r^2 values of 0.78–0.86. Cohen *et al*. (1995) mapped forest cover over 1.3 million ha with an overall accuracy of 82%. Gemmell (1995) distinguished between stand volumes of 150–300 m^3 ha^{-1} in British Columbia, Canada, with 78% accuracy using TM data. Likewise, Olsson (1994) demonstrated the ability to classify thinned and unthinned stands of Scots pine and Norway spruce in Sweden with multispectral indices, also from TM data. The above-cited classifications provide only statistical associations between forest attributes and measured remotely sensed reflectances; thus, they offer little basis for extrapolation to other sites or conditions. Often stand structure and density are best evaluated with a

multivariable approach based on information extracted from a georeferenced database, rather than depending exclusively on what can be inferred from various spectral indices.

Although standing and dead biomass represent the major form in which carbon is stored above ground in forest ecosystems, they are exceedingly hard to quantify from space. Many attempts have been made to estimate this variable with optical sensors and with radar. Unfortunately, all of these sensors, regardless of the wavelengths selected, and the analyses attempted, fail to provide good estimates of standing biomass much beyond 100 Mg dry mass ha^{-1} (Waring *et al*., 1995a). Prototypes for satellite-borne laser altimeters have shown promise in greatly increasing the range over which biomass, as well as other stand characteristics, can be obtained from satellites (Weishampel *et al*., 1996).

V. SPATIALLY EXPLICIT LANDSCAPE PATTERN ANALYSIS

Some regional ecological analyses can be accomplished by evaluating each landscape cell individually. Many ecosystem analyses, however, require information about the size, distance, and characteristics of adjacent cells, necessitating a much more sophisticated landscape description. In general, the more adjacent units affect one another, the more complicated are the analyses. As a result, we must recognize that the scale at which we choose to define individual cells will dictate the degree of detail and complexity of the analysis. Many landscape properties could be computed similarly for a global forest cover map or for a local watershed. At the global level, however, only broad forest classes would be defined, whereas at the local scale, patterns in species distribution and age class structure might be evident if the database provided a sufficient level of detail.

A number of quantitative descriptors have been devised to measure landscape spatial characteristics (Fig. 7.16, Table 7.1). All of these landscape computations are based on the assumption that at some level of spatial resolution, a homogeneous unit of land exists, which is termed a *patch.* Each patch exists within a matrix of other patches, together forming the tapestry of a landscape (Forman, 1995). In forests, a patch is generally equivalent to a stand with a homogeneous mixture of species, ages, sizes, and/or stockings of trees. The delineation of a patch, however, is dependent on the spatial scale and degree of detail specified. A landscape defined in units of square kilometers cannot be discriminated into smaller sized patches.

Once the dimensions and other qualifications of a patch are defined, the geometric analyses required to yield estimates of area, shape, and frequency of occurrence over a specified landscape are easily applied. The *edge* or perimeter of a patch defines the boundary with adjacent patches. A *core area* within each patch may also be defined at some specified distance from the boundary. Various additional geometric properties can be computed, such as the fractal dimension, which relates the perimeter of a patch to its area and represents a measure of the complexity of surrounding boundary.

The population variables defined can relate to any organism present, so each defined patch can be very different for each population on the same landscape. Diversity and dominance indices measure the abundance and proportion of types of patches within the population on the landscape. Diversity measures how many different types of patches

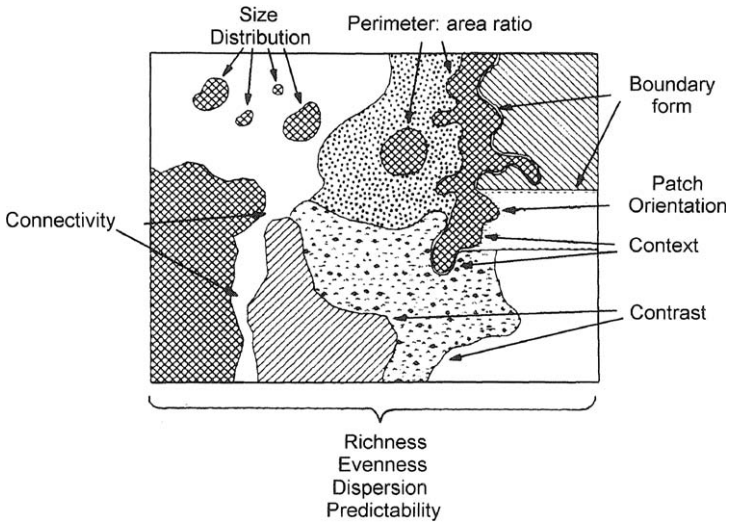

FIGURE 7.16. Hypothetical landscape illustrating various metrics used for quantifying spatial landscape characteristics. Landscape metrics are typically of two types: geometric variables that quantify sizes, shapes, and configuration of land units, and variables that quantify composition, abundance, and locations of populations (McGarigal and Marks, 1995). (Adapted from Wiens *et al*., 1993. © 1993 *Oikos.*)

TABLE 7.1
Types of Quantitative Metrics Computed to Describe Landscape Spatial Characteristics[a]

Metric	Example variables
Geometric variables	
Area	Area in different landscape classes
Patchiness	Patch density, patch size, variability
Edge	Perimeter lengths, densities, contrast
Shape	Fractal dimension
Core area	
Population variables	
Nearest-neighbor	Proximity indices
Diversity	Species richness, diversity indices
Contagion and interspersion	

[a]From FRAGSTATS, McGarigal and Marks (1995).

occur, and dominance measures the proportion of the landscape occupied by each type of patch. FRAGSTATS computes nine different statistical measures of diversity, because there are variable definitions (McGarigal and Marks, 1995). The spatial arrangement of a patch with other patches and degree of regularity of a pattern is measured by proximity (distance to the nearest neighbor), dispersion (the randomness or uniformity of spatial distribution of patches), and contagion indices (clumpiness of patches).

Excellent summaries of these landscape metrics are provided by Turner (1989), Turner and Gardner (1990), Baker (1989), and Naveh and Lieberman (1994). Public domain software packages such as FRAGSTATS developed by McGarigal and Marks (1995) include an assemblage of algorithms required for most of the desired computations. The challenge is to decide which metric best quantifies the ecosystem property of greatest importance to each resource problem. Also, it should be recognized that different metrics when applied to the same problem can lead to divergent interpretations. Regardless, resource managers can, by following landscape changes in time and space, obtain a measure of the success or failure of particular policies, an approach we will explore in some detail in Chapter 8.

VI. DATA LAYER INCONSISTENCIES

An essential part of building databases for regional ecology is the requirement to maintain quality control because data acquired from a myriad of sources will invariably include gaps and unrealistic values. A single error in a huge data layer, such as relative humidity >100%, can prevent the completion of calculations in some ecosystem models. Also, when data are acquired from a variety of sources, inconsistencies will arise that demand cross-comparisons to discard or question values. For example, a soil data set might indicate a water holding capacity of 3 cm for a particular landscape unit, while a vegetation survey will indicate an LAI for the same unit as 12. Independently, both of these values are reasonable, but in combination they are highly unlikely and must he recognized through an automatic screening protocol. One inherent disadvantage of multilayered data sets is the likelihood that many small errors may be embedded in acquired data sets. Special routines are therefore required to find inconsistencies that exist in the geographically registered information on topography, climate, soils, and vegetation before a GIS analysis is initiated.

VII. SUMMARY

To extend our understanding to the landscape and regional level requires different techniques than those appropriate for stand/seasonal studies. The level of detail required depends on the choice of variables and the extent to which they vary spatially. Remote sensing offers an excellent source of georeferenced data but can provide direct information only on a limited suite of variables that alter the reflectance properties of landscapes (spatially, spectrally, temporally, and directionally). Climatological analyses are required to convert information gathered at a dispersed network of weather stations into more relevant forms (radiation, dew point, vapor pressure deficit) and to provide the basis for extrapolation of climatic variation across landscapes. The more time-invariant properties of topography, hydrology, and soils also must be represented spatially. Finally, the extent to which land cover and the type of vegetation vary in both time and space must be presented in a standardized form consistent with the capabilities of sensors, the frequency of satellite coverage, and the cost and difficulty of obtaining and processing digital data. As a consequence of these constraints, landscape ecological models must be developed in concert with what can be directly measured or inferred from remote sensing platforms.

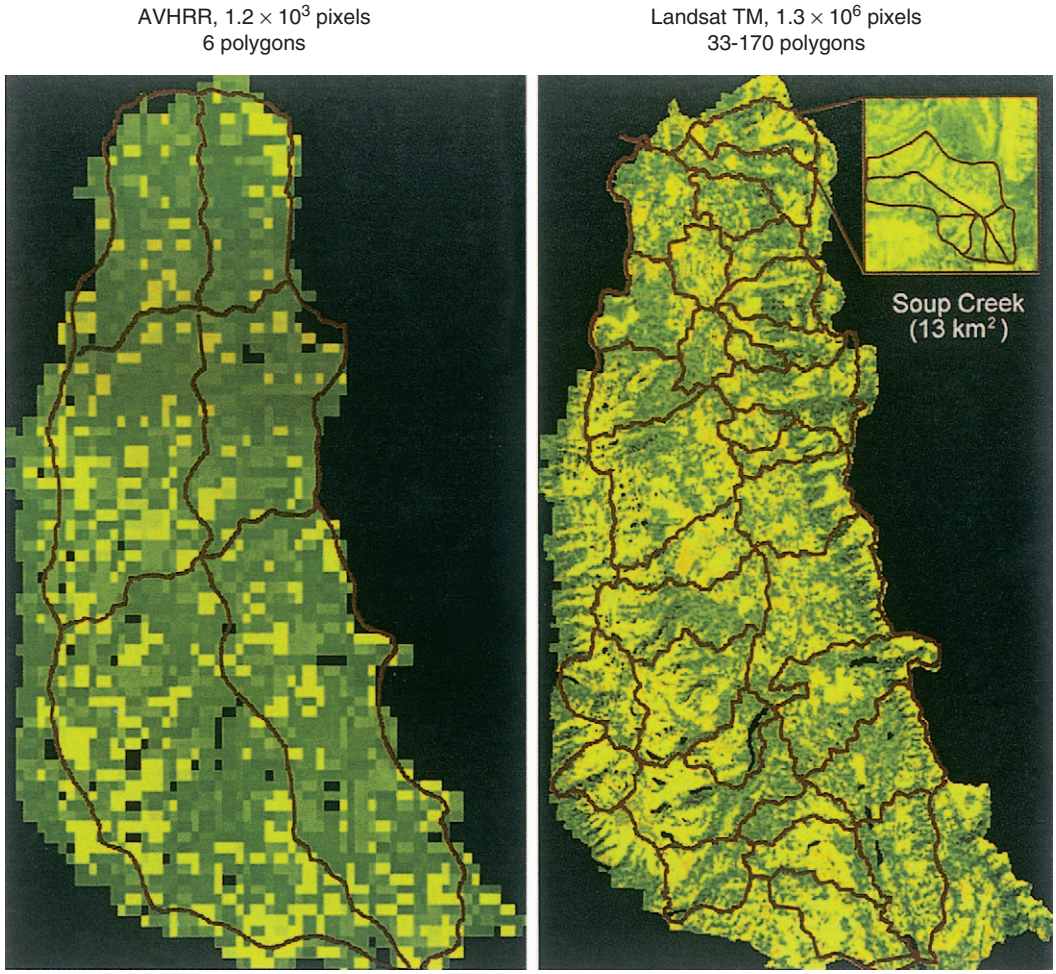

PLATE 1. Principles of landscape partitioning illustrating how digital elevation model (DEM) data can be processed to define the landscape at varying levels of topographic complexity. The Seeley–Swan watershed in Montana is depicted with 1-km^2 raster cells on the left-hand image, 30×30 m resolution cells equivalent to the Landsat pixel size on the right-hand image, and by vector cells defined from topographic analysis with RHESSys (inset). For general regional analyses and averages, the landscape defined with 1-km^2 cells, or six polygons, often provides the most appropriate level of detail to assess the long-term timber harvest potential, watershed yields, and wildlife carrying capacities. For more site-specific decisions, such as the consequences of a specific harvest cycle on other watershed resources, 30×30 m cells or homogeneous polygons that delineate areas <10 km^2 are probably necessary. In general, the more heterogeneous a landscape, the greater is the number of cells required to provide an accurate assessment of spatial variation.

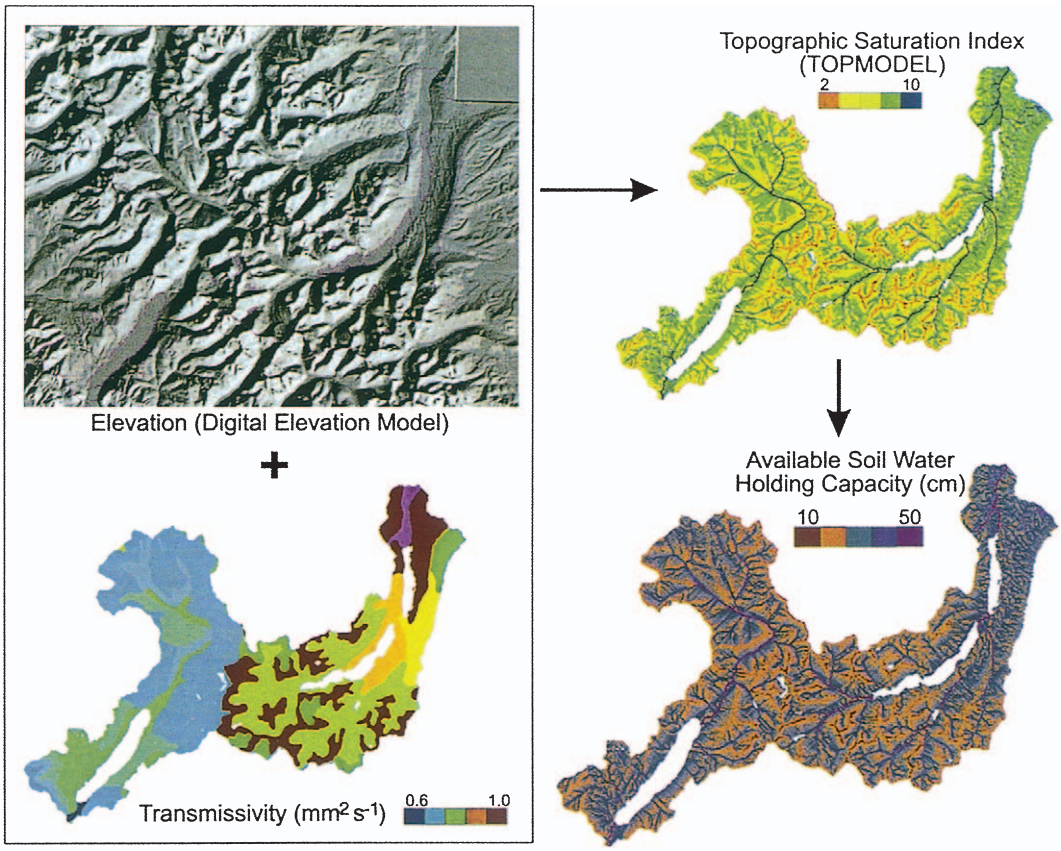

PLATE 2. Steps involved in landscape partitioning based on physical characteristics are demonstrated for the McDonald watershed in Glacier National Park, Montana. First, digital elevation data are combined with a soil water transmissivity data layer derived from soil texture maps and basin delineations and hydrologic drainage networks are computed from the DEM data (Band, 1989a). Then the Topographic Saturation Index (TSI) is computed from TOPMODEL (Beven and Kirkby, 1979). Finally, raw soil textural data are converted to topographically consistent soil water holding capacities in RHESSys following techniques described by Zheng *et al.* (1996). These methods result in data layers that permanently define hydrologic characteristics of a watershed. RHESSys then computes the daily variation in properties for each cell in the watershed, such as precipitation, snowmelt, soil water storage, and evapotranspiration (see Chapter 2).

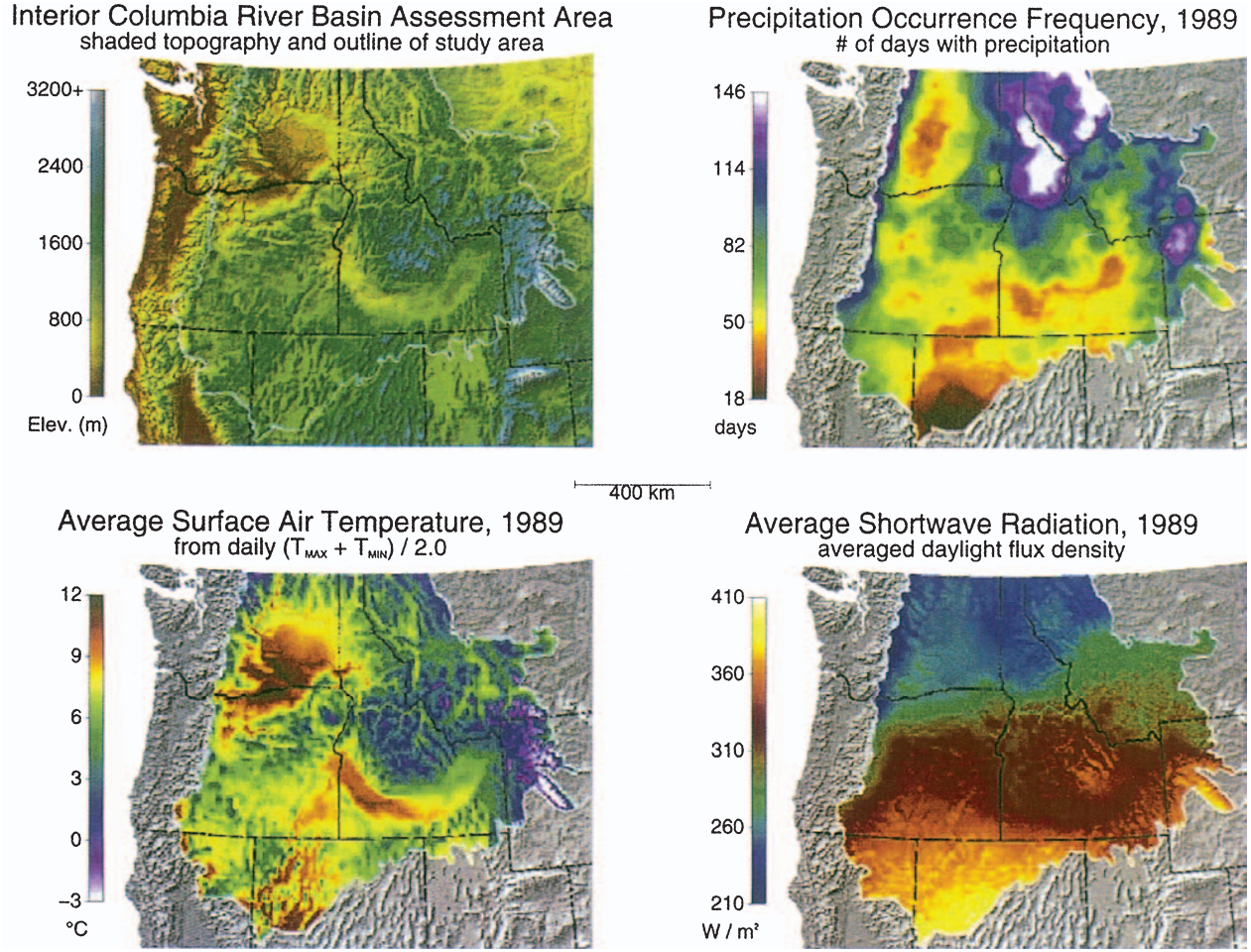

PLATE 3. Example of spatial mapping of annual average daily meteorological conditions for the 820,000-km^2 Columbia River basin in the U.S. Pacific Northwest for 1989 using a three-dimensional version of MT-CLIM called DAYMET (Thornton and Running, 1996; Thornton *et al.*, 1997). Daily air and soil temperature, incident solar radiation, humidity, and precipitation are computed for each cell as part of the RHESSys model, for input into ecological process models such as FOREST-BGC.